Palaeogeography, Palaeoclimatology, Palaeoecology 416 (2014) 92–109

Contents lists available at ScienceDirect

Palaeogeography, Palaeoclimatology, Palaeoecology

journal homepage: www.elsevier.com/locate/palaeo

Isotope compositions (C, O, Sr, Nd) of vertebrate fossils from the Middle Eocene oil shale of Messel, Germany: Implications for their taphonomy and palaeoenvironment

Thomas Tütken *

Steinmann-Institut für Geologie, Mineralogie und Paläontologie, Universität Bonn, Poppelsdorfer Schloss, 53115 Bonn, Germany

ARTICLE INFO

Article history:
Received 15 April 2014
Received in revised form 30 July 2014
Accepted 5 August 2014
Available online 17 August 2014

Keywords:
Strontium isotopes
Oxygen isotopes
Diagenesis
Enamel
Messel
Propalaeotherium

ABSTRACT

The Middle Eocene oil shale deposits of Messel are famous for their exceptionally well-preserved, articulated 47-Myr-old vertebrate fossils that often still display soft tissue preservation. The isotopic compositions (O, C, Sr, Nd) were analysed from skeletal remains of Messel's terrestrial and aquatic vertebrates to determine the condition of geochemical preservation. Authigenic phosphate minerals and siderite were also analysed to characterise the isotope compositions of diagenetic phases. In Messel, diagenetic end member values of the volcanically-influenced and (due to methanogenesis) ^{12}C-depleted anoxic bottom water of the meromictic Eocene maar lake are isotopically very distinct from in vivo bioapatite values of terrestrial vertebrates. This unique taphonomic setting allows the assessment of the geochemical preservation of the vertebrate fossils. A combined multi-isotope approach demonstrates that enamel of fossil vertebrates from Messel is geochemically exceptionally well-preserved and still contains near-in vivo C, O, Sr and possibly even Nd isotope compositions while bone and dentine are diagenetically altered.

Enamel of the hippomorph perissodactyl *Propalaeotherium* has low $\delta^{13}C$ values (-9 ± 0.7‰), typical for C_3-plant-feeders. Dentine of the same teeth has $\delta^{13}C$ values 15–17‰ higher, amongst the highest $\delta^{13}C_{bioapatite}$ values reported for terrestrial vertebrates. This reflects diagenetic carbonate exchange with the strongly ^{12}C-depleted anoxic lake bottom water. Enamel $^{87}Sr/^{86}Sr$ values (~0.711 ± 0.001) are consistent with *Propalaeotherium* feeding on Palaeozoic bedrocks surrounding Lake Messel and suggests that the basaltic tuff ring around the maar was already eroded 640 ka after its formation. Dentine has, however, much lower, volcanically influenced $^{87}Sr/^{86}Sr$ (~0.706) due to diagenetic Sr uptake from the lake water/oil shale. Enamel $\delta^{18}O_p$ values (~18 ± 0.6‰) of *Propalaeotherium* are 2–3‰ lower than those of bones and scales of aquatic vertebrates that lived in the ^{18}O-enriched lake water. Using transfer functions, a $\delta^{18}O_{H_2O}$ value of -5 ± 1‰ for meteoric water and a MAT of ~18 ± 2.5 °C were reconstructed for Messel.

1. Introduction

Messel near Darmstadt in Germany, is a world-famous conservation-Lagerstätte (UNESCO-World Heritage Site) which is renowned for the articulated vertebrate fossils from the middle Eocene lacustrine oil shale deposits, which often have exceptional preservation of soft tissues such as fur, feathers and gut contents (e.g., Schaal and Ziegler, 1992; von Koenigswald et al., 1998; Franzen, 2007; Gruber and Micklich, 2007; Vinter et al., 2010). These vertebrate fossils represent an important window into the evolution of early mammals and other vertebrate taxa, and their palaeobiogeographic distribution and palaeobiology and have thus been extensively studied by palaeontologists over the last 140 years. However, geochemical investigations of these exceptionally well-preserved vertebrate fossils are scarce (Schweizer et al., 2007; Gehler et al., 2011; Herwartz et al., 2013a, b; Pack et al., 2013). Soft tissue remains from aquatic and terrestrial vertebrates are still well-preserved and their carbon and nitrogen isotope compositions were analysed to infer trophic relationships in the Eocene Messel food web (Schweizer et al., 2007). The diagenetic alteration of the oxygen isotope composition in the PO_4-group of bioapatite from a rodent tooth was assessed using triple oxygen (^{16}O, ^{17}O, ^{18}O) isotope analysis. The presence of a negative $\Delta^{17}O$ anomaly in enamel (derived from in vivo inhaled isotopically anomalous air oxygen) demonstrated the preservation of original $\delta^{18}O_p$ values in enamel (Gehler et al., 2011). This $\Delta^{17}O$ anomaly was then used as a proxy to reconstruct the Eocene atmospheric pCO_2 at Messel to 740 ± 430 ppmv, assuming a similar gross primary production as today (Pack et al., 2013). Radiometric Lu–Hf dating of various Messel vertebrate fossils, authigenic siderite and

* Institut für Geowissenschaften, AG Angewandte und Analytische Paläontologie, Universität Mainz, J.-J.-Becherweg 21, 55128 Mainz, Germany. Tel.: +49 6131 3922387.
E-mail address: tuetken@uni-mainz.de.

http://dx.doi.org/10.1016/j.palaeo.2014.08.005
0031-0182/

phosphate minerals as well as oil shale yielded an isochron with an age of 43 ± 19 Ma (Herwartz et al., 2013a). This age roughly corresponds with the stratigraphic age of ~47 Ma for the oil shale (Franzen, 2005; Mertz and Renne, 2005), however, the large isochron error (due to low sample Lu/Hf ratios) hinders extraction of a useful age from the data. High Hf contents and unusual intra-bone REE fractionation profiles indicate special taphonomic processes in Messel (Herwartz et al., 2013a, b). Overall these geochemical data indicate a good preservation of vertebrate fossils from Messel.

The isotope compositions of bioapatite from vertebrate hard tissues such as bones, teeth and scales contain a wealth of information about diet, climate, palaeoenvironment and habitat use of animals (see reviews in Kohn and Cerling, 2002; Koch, 2007; Tütken, 2010). However, diagenesis may alter in vivo isotope signatures in vertebrate fossils, and is best evaluated using a variety of approaches (Kohn et al., 1999; Tütken and Vennemann, 2011 and references therein). The special taphonomic conditions (bottom water anoxia and meromixis) of Lake Messel caused an exceptional preservation of soft tissues (Wuttke, 1983, 1992; Vinter et al., 2010; McNamara et al., 2012) and molecular fossils such as biomarkers (Kimble et al., 1974; Chappe et al., 1982; Hayes et al., 1987), also suggest favourable conditions for the preservation of phosphatic hard tissues and in vivo isotope signatures. Herein I attempt to assess whether the (macroscopically) exceptionally well-preserved vertebrate fossils of Messel are also geochemically well-preserved. If in vivo stable isotope compositions of bones and teeth are preserved, these will be used to infer the palaeobiology and palaeoenvironmental surroundings of some middle Eocene vertebrates, with a special focus on the terrestrial hippomorph perissodactyl *Propalaeotherium*. For this purpose, a multi-isotope (C, O, Sr, Nd) approach was used to analyse fossil bones and teeth both of terrestrial and aquatic vertebrates from Messel. Additionally authigenic mineral phases such as messelite ($Ca_2(Fe^{2+},Mn)(PO_4)_2 \cdot 2H_2O$), montgomeryite ($Ca_4MgAl_4(PO_4)_6(OH)_4 \cdot 12H_2O$) and siderite ($FeCO_3$), commonly forming encrustations around vertebrate fossils, were analysed to characterise these diagenetic phases isotopically. This will yield new geochemical information about the taphonomic conditions and fossilisation processes of vertebrate remains as well as the palaeoclimatic and palaeoenvironmental conditions in and around Lake Messel.

2. Lake Messel: geological, palaeoenvironmental and taphonomic setting

2.1. Bedrock geology and maar formation

The Messel pit, a former oil shale open cast mine, is situated 10 km NE of Darmstadt (Hesse State, Germany) situated on the Sprendlinger Horst, an uplifted Palaeozoic basement block (Fig. 1A). The Sprendlinger Horst is formed by crystalline rocks of Carboniferous to lower Permian age that are partially covered by Upper Permian (Rotliegend) siliciclastic sediments composed of reworked plutonic basement rocks (Marell, 1989; Harms et al., 1999; Mezger et al., 2013). During the Eocene a major phase of volcanic activity with basaltic effusions occurred on the Sprendlinger Horst (49 to 47 Ma; Mertz and Renne, 2005). The Eocene volcanism occurred presumably along tectonic faults (Mezger et al., 2013) and formed several isolated volcanic and tectonic basins, including Messel (Harms et al., 1999; Felder and Harms, 2004). The Grube Prinz von Hessen oil shale deposit, however, is not of volcanic origin and is, at the minimum, 2 Ma younger than Messel (Franzen, 2006). All these sedimentary basins were filled with Eocene lacustrine siliciclastic sediments (Weber and Hofmann, 1982; Harms et al., 1999; Franzen, 2006).

The volcanic origin of Messel as a maar was already postulated by Hummel (1924) and Rietschel (1994) but only unambiguously confirmed in 2001 by a 433 m long research drill core (Messel FB 2001, Fig. 1B). FB 2001 penetrated through the Middle Eocene sedimentary sequence of oil shales and siliciclastic lake sediments (0–228 m) of the middle and lower Messel Formation, the lapilli tuff (228–373 m) and into the diatreme breccia (373–433 m) forming the crater infill (Felder and Harms, 2004, Fig. 1B). The maar formation has been $^{40}Ar/^{39}Ar$ dated to 47.8 ± 0.2 Ma using a basalt fragment from the pyroclastic lapilli tuff sequence below the oil shale (Mertz and Renne, 2005). The diatreme formed within felsic and mafic plutonic rocks (granite, granodiorite, diorite) of Carboniferous and Lower Permian age along the Messel Fault Zone that acted as pathway for the ascent of Palaeogene basaltic magma (Mezger et al., 2013). The lack of any Mesozoic clasts in the diatreme breccia indicates that the Eocene land surface around Messel was made up of Permian and/or Carboniferous rocks while Triassic sedimentary cover rocks were already eroded away (Felder and

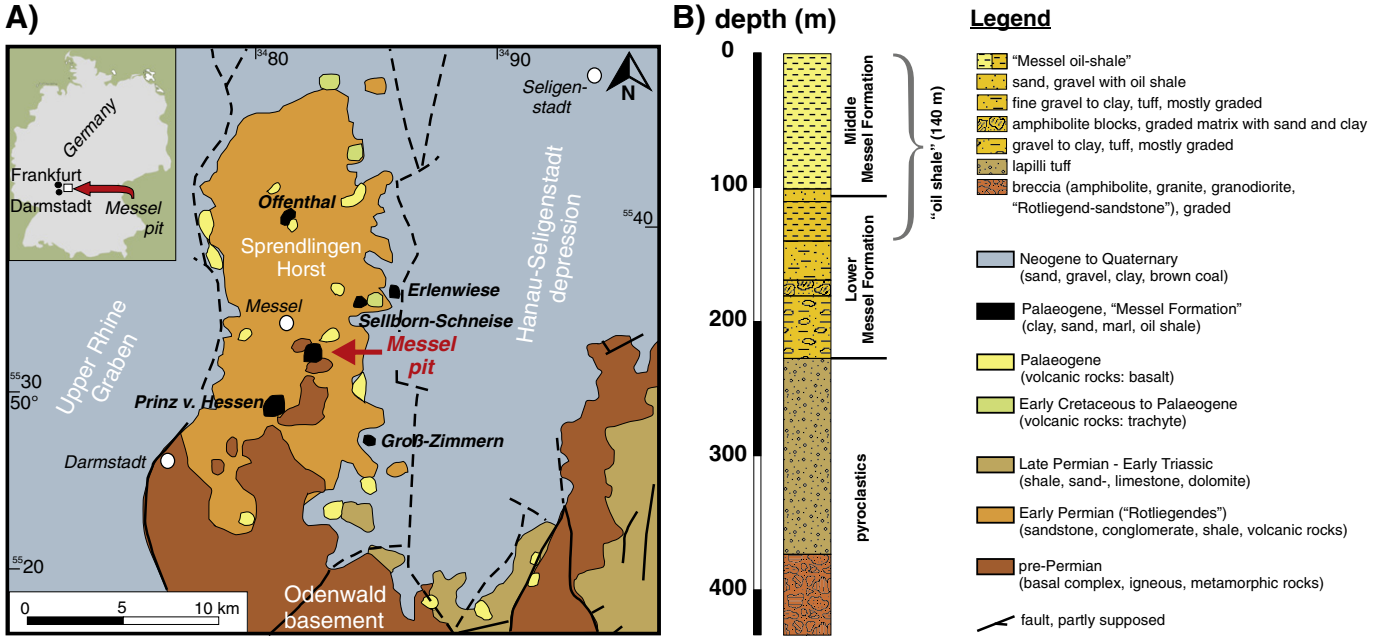

Fig. 1. A, Geological map showing the location of the Messel pit in relation to other Palaeogene sites on the Palaeozoic basement of the Sprendlinger Horst (modified after Lenz et al., 2011 based on Harms et al., 1999). B, Generalised section of the Messel 2001 core (after Felder and Harms, 2004) displaying the major lithological units.

Harms, 2004). The uplift of the Sprendlinger Horst since the middle Oligocene presumably caused little erosion (i.e. less than 50–100 m) of the Eocene land surface (Harms et al., 1999). This and the sheltered position of the lake deposits in the maar, as well as the subsidence of the diatreme infill, led to the preservation of the Messel oil shale and the extraordinary vertebrate remains embedded therein.

2.2. Lake Messel: hydrology, oil shale formation and sedimentation rates

The diatreme was filled with a maar lake that was about 1 km in diameter and, initially, more than 300 m deep. Whether or not the lake had permanent fresh water inflow is still a matter of discussion. An inflow of a small stream from the NW and weak water currents were postulated based on sedimentological arguments and the orientation and size sorting of vertebrate carcasses (Franzen et al., 1982; Franzen, 2007). Recurrent connections to a river network are indicated by the fish fauna in the lake (Micklich, 2012). In its early phase debris flows from collapsing crater walls led to the re-sedimentation of volcanoclastic material with intercalated oil shale layers (Felder and Harms, 2004). After the stabilisation of the crater walls the holomictic Lake Messel became permanently meromictic (Goth, 1990; Lenz et al., 2007) and developed extremely anoxic bottom water conditions with methanogenesis. Methane formation in Lake Messel is indicated by extensive formation of authigenic siderite with very positive $\delta^{13}C$ values (Bahrig, 1989; Felder and Gaupp, 2006) and biomarkers of methanogenic bacteria (Chappe et al., 1982; Hayes et al., 1987). Anoxic bottom water led to the deposition of mostly laminated, bituminous (on average ~27 wt.% C_{org}; Bauersachs et al., 2014) and water-rich black pelites ("oil shale") forming a 228 m thick sequence of the Messel Formation on top of the pyroclastic diatreme infill (Felder and Harms, 2004). The lower Messel Formation is predominantly composed of siliciclastic lake sediments with intercalated oil shales while the middle Messel Formation is mostly composed of laminated oil shale (Matthess, 1966; Felder and Harms, 2004, Fig. 1B). The clay fraction of the oil shale is mostly smectite, a weathering product of the basaltic tuff material, and lesser amounts of illite and kaolinite (Weber, 1991). The organic material in the oil shale is mostly consisted of cell wall remains of the coccal green algae *Tetraedron*, forming varves of clay-rich darker and *Tetraedron*-rich lighter laminae (Goth, 1990). However, the organic matter of the Messel oil shale is not only derived from different autochthonous, aquatic primary producers such as phytoplankton, prokaryotes and algae, but a variable yet significant fraction also comes from terrestrial vascular plants (Bauersachs et al., 2014). A maximum thickness of 91.5 m laminated oil shale of the Middle Messel Formation preserved at the site of the research drill core represents about 640,000 years calculated from an average sedimentation rate of 0.14 mm/yr (Lenz et al., 2010). Sedimentation rates of about 0.1 to 0.15 mm/yr estimated from varve counts of the laminated oil shale indicate that Lake Messel existed >640 ka (Lenz et al., 2010) up to about 1 Ma (Goth, 1990). It is the upper portions of the laminated oil shales of the middle Messel Formation that contain the well-preserved fossils that are analysed in this study (Fig. 1B).

2.3. Messel fossils: taphonomy and exceptional preservation

Anoxic bottom water along with a lack of bioturbation and reduced degradation by anaerobic microbes led to the undisturbed deposition of macrofossils of vertebrates at Messel (Schmitz, 1991; Schaal and Ziegler, 1992; von Koenigswald and Storch 1998; Franzen, 2007; Gruber and Micklich, 2007; Mayr, 2009; Joyce et al., 2012; Micklich, 2012; Schwermann et al., 2012; Smith and Wuttke, 2012), plants (Wilde, 1989, 2004; Collinson et al., 2012) and invertebrates (Neubert, 1999; Wedmann, 2005), as well as microfossils such as pollen and spores (Thiele-Pfeiffer, 1988; Lenz et al., 2007, 2011), algae (Goth, 1990; Lenz et al., 2007) and sponge spicules and gemmules (Richter and Wuttke, 1999; Richter and Baszio, 2009). The preservation of the fossils is exceptional with beetles still displaying structural colours (McNamara et al., 2012); feathers featuring preserved arrays of fossilised melanosomes, allowing reconstruction of the original colouration (Vinter et al., 2010); and plant macrofossils preserved as remnants of the original organic material in various stages of compression and degradation (Wilde, 1989; Collinson et al., 2012). Furthermore, molecular fossils, such as biomarkers of algae, bacteria and higher plants, are preserved in the kerogen fraction of the oil shale (Kimble et al., 1974; Michaelis and Albrecht, 1979; Michaelis et al., 1988; Chappe et al., 1982; Hayes et al., 1987).

The Messel vertebrate fossils, in particular the articulated carcasses of 46 mammal species are world famous. Often preserved with soft tissue preservation (Wuttke, 1983, 1992) and gut contents (Sturm, 1978; von Koenigswald and Schaarschmidt, 1983; Richter and Storch, 1994), these exceptional fossils represent a unique window into the evolution of early mammals (von Koenigswald and Storch 1998; Franzen, 2007; Rose, 2012). These fossils belong to the Mammal Paleogen biostratigraphic reference level MP 11 in the lower Geiseltalian European Land Mammal Age and are approximately 47 Ma old (Franzen, 2005; Mertz and Renne, 2005). The fossiliferous oil shales were only exposed to burial temperatures of less than 40 °C (Kimble et al., 1974; Hayes et al., 1987) and have a very low degree of kerogen maturation (Bauersachs et al., 2014) and thus a low average vitrinite reflectance of 0.26% (Michaelis et al., 1988; Rullkötter et al., 1988). Post-Eocene sediment cover that has overlain the oil shales of the Messel Formation was limited to <100 m. This explains the extraordinary preservation of molecular, plant and animal fossils embedded in the oil shale.

2.4. Eocene palaeogeography and palaeoclimate of Lake Messel

During the Middle Eocene Messel was at a somewhat more southerly latitude because the European plate has moved approximately 3 to 4°N north over the last 47 Ma. Messel was palaeogeographically situated in the middle of the central European land mass with the coastline of the North Sea being about 400 km away (Kockel, 1988). The fossiliferous oil shale was deposited under a paratropic, warm and humid climate with some seasonality (Wilde, 1989; Grein et al., 2011a). Mean annual temperatures (MAT) have been inferred from plant macro- and micro-fossils using a coexistence approach (CA) at the family level and leaf margin analysis (LMA), ranging from 16.8 to 23.9 °C and 21.7 to 23.1 °C, respectively, with an overall MAT ~22 °C (Grein et al., 2011a). Coldest month temperatures were well above 10° (Grein et al., 2011a), which is further supported by the presence of thermophilic reptiles such as crocodiles (Berg, 1964; Markwick, 1998). Mean annual precipitation of around 2540 mm and a relative humidity of 75 ± 2% were reconstructed using the CA (Grein et al., 2011a). Atmospheric pCO_2 levels at Messel were about 3–4 times higher than today 740 ± 430 ppmv (Pack et al., 2013; based on $\Delta^{17}O$ anomaly in rodent enamel bioapatite) to 853–1033 ppmv (Grein et al., 2011b; using stomata densities and a plant physiological model). Overall a subtropical climate with some seasonality in rainfall and temperature similar to a Cfa type climate, such as that found today in the Yunnan Province, China, prevailed in Messel 47 Ma ago (Grein et al., 2011a).

3. Background C, O and Sr isotopes: proxies for diet, climate and habitat

A multi-isotope approach was applied to test whether still in vivo isotope signatures are preserved in 47 Ma-old bioapatite of Messel vertebrate fossils. For this purpose skeletal tissues more or less prone to diagenetic alteration (enamel ≪ dentine < bone) as well as skeletal remains from different terrestrial and aquatic vertebrates with distinct diet and habitat were analysed. The stable isotope compositions (C, O, Sr, Nd) incorporated by the vertebrates in vivo are expected to be distinct from those taken up post mortem because of the specific hydrologic and geologic conditions in and around Lake Messel. Large differences

can be anticipated, for example, in carbon isotope ratios, with low $\delta^{13}C$ values in terrestrial C_3 plants compared to the high $\delta^{13}C$ values expected in dissolved inorganic carbon (DIC) in lake water due to anoxia and methanogenesis (Bahrig, 1989; Felder and Gaupp, 2006). Differences would also be expected in strontium as the Palaeozoic bedrocks forming the basement around the Messel maar have radiogenic $^{87}Sr/^{86}Sr$ ratios compared to the unradiogenic $^{87}Sr/^{86}Sr$ in the lake water and oil shale, which are derived from the weathering of the basaltic Eocene pyroclastics. The lake existed over 640 ka (Lenz et al., 2010) and is assumed to have been mostly isolated from the hydrographic network (e.g. Goth, 1990). However, a recent study of the fish fauna suggests at least occasional connections to a river network during high water periods (Micklich, 2012). By analysing bioapatite $\delta^{18}O_p$ values of terrestrial and aquatic vertebrates it will be tested if the Messel Lake had ^{18}O-enriched water compared to local precipitation.

Because expected biogenic and diagenetic end member values for the bioapatite of terrestrial vertebrates and authigenic phosphate minerals forming from the pore water are so distinct, Messel provides a unique geological and taphonomic setting to test for diagenetic alteration of vertebrate skeletal remains. Where original isotope signatures are preserved, these could be used to infer the diet, drinking water and habitat of Messel vertebrates as well as climatic conditions such as air and water temperature. In the following a brief overview will be given explaining how the different isotope systems can be used for these purposes.

3.1. Carbon isotopes ($\delta^{13}C$ values)

Bioapatite of bones and teeth contains a small amount of structural carbonate (CO_3) substituting on the A site (for PO_4 ~ 90%) and B site (for OH ~10%) in the apatite crystal lattice (Pasteris et al., 2008). The carbon isotope composition of the carbonate ($\delta^{13}C_{CO_3}$) in bioapatite reflects the $\delta^{13}C$ value of the bulk diet (DeNiro and Epstein, 1978; Ambrose and Norr, 1993). Bioapatite in consumers is enriched in ^{13}C compared to the diet and $\varepsilon_{diet-apatite}$ enrichment factors range from 9 to 14‰, depending on taxon, diet and digestive physiology (Passey et al., 2005). Large herbivorous ungulates have $\varepsilon_{diet-apatite}$ of 14‰ (Cerling and Harris, 1999). Thus enamel of herbivores records $\delta^{13}C$ values of ingested food plants, which enables the reconstruction of diet and niche behaviour. For example, plant $\delta^{13}C$ varies according to taxonomy, specific plant tissue, and growth habitat of the plant (e.g., shade versus full sun). Furthermore, C_3 and C_4 plants (mostly grasses) use distinct photosynthetic pathways and have a significant isotopic difference of about 14‰ (Farquhar et al., 1989). This enables dietary reconstructions of fossil vertebrates and to distinguish grazers from browsers (Cerling et al., 1997; MacFadden et al., 1999) and thus vertebrates feeding in open C_4 grasslands versus closed C_3 forested habitats. This allows to infer type and density of vegetation cover. However, as C_4 plants have been globally abundant only since late Miocene time (~7 to 8 Ma; Cerling et al., 1993, 1997), and C_4 grasslands never evolved in Europe, the carbon isotope distributions in Messel fossils are expected to reflect purely C_3 vegetation, and any subsequent diagenetic overprinting. Prior to Miocene times, only niche partitioning within C_3 plant ecosystems can be reconstructed (e.g., MacFadden and Higgins, 2004; Feranec and MacFadden, 2006; Tütken and Vennemann, 2009). The carbon isotope fractionation of C_3 plants is affected by environmental and climatic factors such as aridity, light availability, and vegetation density (Heaton, 1999; Diefendorf et al., 2010; Kohn, 2010). This enables the identification of vertebrates feeding in densely forested areas as they have ^{13}C depleted bioapatite $\delta^{13}C$ signatures (van der Merwe and Medina, 1991; Cerling et al., 2004) compared to herbivores feeding in more open habitats. Along the food chain only a slight enrichment in ^{13}C occurs so that carnivores have only slightly higher $\delta^{13}C$ values compared to their herbivore prey (Kohn et al., 2005; Fox-Dobbs et al., 2006). Tooth enamel can preserve its original carbon isotope composition over millions of years (Lee-Thorp and van der Merwe, 1987; Fricke et al., 2008) and $\delta^{13}C$ values are widely applied in palaeontology to infer the diet of extinct vertebrates. Previous studies at Messel have analysed organic carbon and nitrogen isotope compositions of soft tissue remains of some vertebrates, demonstrating remarkable preservation, and inferring past dietary habits and food web relationships (Schweizer et al., 2007). Here it will be assessed whether dietary $\delta^{13}C$ signatures are also preserved in the carbonate of skeletal apatite of vertebrates from Messel.

3.2. Oxygen isotopes ($\delta^{18}O$ values)

Oxygen isotopes of vertebrate bioapatite, both of carbonate ($\delta^{18}O_c$) and phosphate ($\delta^{18}O_p$), are a proxy for $\delta^{18}O$ values of ingested meteoric or ambient water (Longinelli, 1984; D´Angela and Longinelli, 1990; Delgado Huertas et al., 1995; Kohn, 1996; Amiot et al., 2004, 2007). Bioapatite $\delta^{18}O$ signatures are controlled by body temperature, drinking water and food water as well as inhaled air oxygen (Bryant and Froelich, 1995; Kohn, 1996). For endothermic terrestrial mammals, body temperature, and therefore the oxygen isotope equilibrium fractionation between the body water and bioapatite, is constant and bioapatite $\delta^{18}O$ values are mainly controlled by ingested meteoric water (Longinelli, 1984; Luz et al., 1984; Luz and Kolodny, 1985). The same applies for certain ectotherm vertebrates such as crocodilians and aquatic turtles that only mineralise bioapatite of their bones and teeth in a narrow temperature window (Barrick et al., 1999; Amiot et al., 2007). There are various empirical regressions between $\delta^{18}O_p$ of bone and tooth apatite for endotherm mammals (e.g., Longinelli, 1984; Delgado Huertas et al., 1995; Amiot et al., 2004) but also for aquatic ectotherm vertebrates such as crocodilians (Amiot et al., 2007) and turtles (Barrick et al., 1999). For terrestrial and limnic taxa, $\delta^{18}O_{H_2O}$ values of drinking water and ambient water, respectively, can be inferred using these equations (Table 1). Air temperatures can be calculated using modern-day relations between air temperature and $\delta^{18}O_{H_2O}$ of meteoric water (e.g., Rozanski et al., 1993; Fricke and O'Neil, 1999; Amiot et al., 2004), because $\delta^{18}O_{H_2O}$ of precipitation is, beside amount, altitude and continentality effects predominantly controlled by air temperature during rainout (Dansgaard, 1964; Rozanski et al., 1993, 1997). However, surface waters can be modified by evaporation processes or advection/mixing with waters, which can lead to ^{18}O enrichment, especially in longterm lakes (Talbot, 1990) such as Lake Messel. Water

Table 1
Calibrations between $\delta^{18}O_{H_2O}$ and vertebrate $\delta^{18}O_{PO_4}$ as well as ambient temperature.

Taxon	Equation	Equation nr.	Reference
Aquatic turtles[a]	$\delta^{18}O_{H_2O} = 0.994 * \delta^{18}O_{PO_4} - 21.197$	1	Pouech et al. (2014)
Crocodilians	$\delta^{18}O_{H_2O} = 0.823 \pm 0.247 * \delta^{18}O_{PO_4} - 19.129 \pm 4.183$	2	Amiot et al. (2007)
Rodents	$\delta^{18}O_{H_2O} = 1.75 * \delta^{18}O_{PO_4} - 36.68$	3	Navarro et al. (2004)
Horse	$\delta^{18}O_{H_2O} = 1.40 * \delta^{18}O_{PO_4} - 31.83$	4	Delgado Huertas et al. (1995)
Mammals	$\delta^{18}O_{H_2O} = 1.113 \pm 0.003 * \delta^{18}O_{PO_4} - 26.441 \pm 0.051$	5	Amiot et al. (2004)
Temperature (water)	$T(°C) = 117.4 \pm 9.5 - 4.50 \pm 0.43 * (\delta^{18}O_{PO_4} - \delta^{18}O_{H_2O})$	6	Lécuyer et al. (2013)
Temperature (air)	$T(°C) = 2.041 \pm 0.06 * \delta^{18}O_{H_2O} - 28.938 \pm 1.06$	7	Amiot et al. (2004)

[a] Note this is the regression of Barrick et al. (1999) recalculated to a value of 21.7‰ for the NBS 120c taken from Pouech et al. (2014).

temperatures can be reconstructed from $\delta^{18}O_p$ values of fish teeth and bones (Kolodny et al., 1983) using phosphate–water oxygen isotope fractionation equations (Longinelli and Nuti, 1973; Lécuyer et al., 2013; Table 1). This approach will be applied for fish bones and scales from Messel using a lake water $\delta^{18}O_{H_2O}$ value reconstructed from $\delta^{18}O_p$ values of aquatic turtle bones and crocodile teeth.

3.3. Strontium isotopes ($^{87}Sr/^{86}Sr$)

Strontium isotopes are widely applied as an isotopic fingerprint of the bedrock substrate in ecology, archaeology and palaeontology (Blum et al., 2000; Bentley, 2006; Tütken et al., 2006, 2011). $^{87}Sr/^{86}Sr$ ratios vary between different rocks because ^{87}Rb decays to ^{87}Sr with a half life of 48 Ga. Thus depending on the Rb/Sr ratio and age of the rock $^{87}Sr/^{86}Sr$ ratios differ in rocks of different lithology and geologic age. Old crustal rocks have high $^{87}Sr/^{86}Sr$ of >0.711 and young mantle-derived volcanic rocks have ratios around 0.703 while marine carbonates have intermediate values of 0.707 to 0.709 (depending on geological age; McArthur et al., 2001). Strontium is released by weathering processes from the rocks/minerals to the environment and enters as bioavailable Sr via plant uptake into the food chain (e.g., Blum et al., 2000). Strontium is mostly ingested with the food and subordinate amounts with the drinking water. It is a non-essential trace element that is biopurified along the food chain (Balter, 2004 and references therein). Unlike light stable isotopes such as C and O, $^{87}Sr/^{86}Sr$ is not significantly fractionated during metabolism, tissue formation and biomineralisation. Thus bioavailable Sr isotope signatures are incorporated from the environment unchanged into bioapatite of bones and teeth (Price et al., 2002; Maurer et al., 2012). Therefore $^{87}Sr/^{86}Sr$ can be used to distinguish local from non-local individuals and detect habitat use (Beard and Johnson, 2000; Feranec et al., 2007; Arppe et al., 2009; Copeland et al., 2011) migration between isotopically distinct geological domains (Sillen et al., 1998; Hoppe et al., 1999; Blum et al., 2000; Britton et al., 2009, 2011; Tütken et al., 2011) as well as the migration histories of individuals (Hoppe et al., 1999; Müller et al., 2003; Schweissing and Grupe, 2003; Balter et al., 2008). Here $^{87}Sr/^{86}Sr$ ratios are used to characterise the habitat (i.e. bedrock substrate, lake water) of the different terrestrial and aquatic vertebrates of Messel as well as diagenetic Sr uptake from the pore water.

4. Material and methods

4.1. Bioapatite as well as authigenic phosphate and siderite samples

Skeletal remains (bones, teeth, scales) of two terrestrial vertebrates (*Propalaeotherium hassiacum*, *Kopidodon macrognathus*) and five aquatic vertebrates (fish: *Atractosteus messelensis*, *Amphiperca multiformis*, *Cyclurus kehreri*; crocodiles: *Diplocynodon darwini* and turtles: *Allaeochelys crassesculpta*) as well as several phosphatic coprolites were analysed for their stable isotope compositions (Table 2). Except for the six *Propalaeotherium* teeth from the collection of the Hessisches Landesmuseum in Darmstadt (HLMD) all other samples were taken from freshly excavated fossils from excavation campaigns of the years 2007, 2008 and 2011 by the Senckenberg Messel research division (SMF). Fossils were excavated in different stratigraphical levels of the upper middle Messel Formation: excavation area E8/9 in a depth between 150 and 450 cm above the marker horizon alpha and excavation area i14 in a depth of 95 to 175 cm above marker horizon M (montgomeryite) (for stratigraphic position of marker beds see Schaal et al., 1987; Neubert, 1999). Enamel and dentine from two *Propalaeotherium* teeth were analysed to check for the degree of diagenetic alteration by comparing isotope signatures of the two dental tissues, with dentine being more prone to diagenetic alteration than enamel. To characterise the isotopic composition of the diagenetic pore fluid, authigenic phosphate minerals such as montgomeryite (from marker bed M) and messelite (from the "double messelite horizon"; Neubert, 1999) as well as siderite ($FeCO_3$), the latter often forming diagenetic crusts around fossils, were also analysed.

4.2. Rock, water and wood samples

Rock and modern wood samples from the Messel pit were sampled to characterise the $^{87}Sr/^{86}Sr$ biologically available ('bioavailable') to the vertebrates on the Eocene land surface in the surrounding of Lake Messel. Rock samples were taken from the FB 2001 Messel research drill core (Felder and Harms, 2004) and comprise several oil shale samples, a silty lake sediment, a lapilli tuff as well as the basalt fragment, which was Ar–Ar dated to determine the radiometric age of Messel (Mertz and Renne, 2005). Additional various Palaeozoic plutonic and sedimentary rocks were sampled from several other drill cores (GA 1, GA 2, TB 2, IN 25) around the Messel pit and Eocene lacustrine sediments from the neighbouring Grube Prinz von Hessen oil shale exposure (Table 4). All rock samples were taken from the sediment core storage site of the Messel pit. Additionally the embedding oil shale and siderite of one crocodile (FK KR ME 1) and one turtle (FK SCH ME 2) were analysed (Table 3). The wood samples from branches of six trees (*Fagus silvatica*, *Quercus robur*, *Betula pendula*) growing on different bedrock substrates (oil shale, granite, diorite, Permian sediments) were collected in the Messel pit in June 2008 (Table 5). Finally one groundwater sample from the well of the Messel FB 2001 research drill hole was analysed for its strontium isotope composition (Table 4).

4.3. Carbon and oxygen isotope analysis of carbonate

Ten milligrams of bioapatite (enamel, dentine, scale) was pretreated with NaOCl for 3 h and 0.1 M suprapure acetic acid for 10 min to remove organics and diagenetic carbonate. In between the treatments sample powders were rinsed 4 times with MilliQ water. Of the dried pretreated powders about 2 mg was analysed using a Thermo Gasbench II coupled via a Conflo II to a DeltaPlus XL gas mass spectrometer at the University of Tübingen. Precision of $\delta^{13}C$ and $\delta^{18}O$ analysis of the carbonate in the bioapatite was better than 0.1‰ and 0.15‰, respectively.

4.4. Phosphate oxygen isotope analysis

Four milligrams of the pretreated sample powders was dissolved in 0.8 ml 2 M HF overnight. After centrifugation the supernatant solution was transferred to a new 2 ml safe lock centrifuge vial, neutralised with NH_4OH until the added Bromthymol blue pH indicator turned greenish-blue (pH 7–8). Then 0.8 ml of 2 M $AgNO_3$ solution was added for a fast precipitation of Ag_3PO_4. After removal of the supernatant the silver phosphate crystals were washed 4 times with MilliQ water and oven dried at 50 °C. Aliquots of 500 μg each were weight into silver capsules for triplicate phosphate oxygen isotope ($\delta^{18}O_p$) analysis. Samples were analysed using a Finnigan TC/EA for pyrolysis at 1450 °C. The He carrier-CO sample gas was passed through a Mg-perchlorate water trap and then routed through a 1/8 inch steel capillary immersed in liquid nitrogen to trap phosphorous prior entering a Conflo II and oxygen isotope analysis of the purified CO was performed on as DeltaPlus XL gas mass spectrometer at the University of Tübingen. Raw $\delta^{18}O_p$ values were normalised using a regression of several standards (TU1, TU2) according to the values and method given in Vennemann et al. (2002). The precision of $\delta^{18}O_p$ analysis was ±0.3‰. NBS 120c prepared along with samples and analysed in the same runs yielded a $\delta^{18}O_p = 21.8 \pm 0.3‰$ ($n = 12$). This value is in agreement with the 21.7‰ value reported in the early nineties by Lécuyer et al. (1993) and subsequently confirmed by many other laboratories (summarised in the appendix of Chenery et al. (2010)). This value differs, however, from the value of 22.6‰ reported by Vennemann et al. (2002) obtained by fluorination with BrF_5 and similar values around 22.5‰ from a few other labs. Ongoing re-assessment by Vennemann in the Lausanne stable isotope laboratory using different analytical

Table 2
Isotope compositions (C, O, Sr) of bioapatite samples of Messel.

Sample-Nr.	Taxon	Material	Skeletal element	Specimen-nr.	Excavation site–find-nr.	Stratigraphic level	δ^{13}CVPDB	SD	$\delta^{18}O_{CO_3}$ (‰ VPDB)	SD	$\delta^{18}O_{CO_3}$ (‰ VSMOW	$\%CO_3$	$\delta^{18}O_{PO_4}$ (‰ VSMOW)	SD	$^{87}Sr/^{86}Sr$	SD (ppm)
FZ EQ ME 1	*Propalaeotherium hassiacum*	Enamel	M	HLMD ME 144	ND	ND	−8.6	0.1	−4.6	0.1	26.2	4.2	17.8	0.2	0.71142	9
FD EQ ME 1	*Propalaeotherium hassiacum*	Dentine	M	HLMD ME 144	ND	ND	8.7	0.0	−3.5	0.0	27.3	5.7	18.3	0.3	0.70567	9
FZ EQ ME 2	*Propalaeotherium hassiacum*	Enamel	M3 sin	HLMD ME 144	ND	ND	−9.6	0.1	−4.9	0.1	25.9	3.4	17.6	0.3	0.70972	18
FZ EQ ME 3	*Propalaeotherium hassiacum*	Enamel	M	HLMD ME 5332a	ND	ND	−8.6	0.2	−4.5	0.1	26.3	3.2	18.6	0.4	0.71093	6
FZ EQ ME 4	*Propalaeotherium hassiacum*	Enamel	M2	HLMD ME 82	ND	ND	−8.6	0.1	−6.1	0.1	24.6	3.4	17.4	0.4	0.70713	7
FZ EQ ME 5	*Propalaeotherium hassiacum*	Enamel	M	HLMD ME 79	ND	ND	−7.8	0.1	−4.0	0.1	26.8	3.0	19.0	0.3	0.71108	19
FD EQ ME 6	*Propalaeotherium hassiacum*	Dentine	M3	HLMD ME 144	ND	ND	5.6	0.1	−3.6	0.1	27.2	5.1	20.0	0.3	0.70598	6
FZ EQ ME 6	*Propalaeotherium hassiacum*	Enamel	M3	HLMD ME 144	ND	ND	−9.8	0.1	−4.8	0.1	26.0	3.3	18.1	0.4	0.71199	19
FK KOP ME 1	*Kopidodon macrognathus*	Bone		SMF ME 11399	F9–7178	250–350 cm above α	ND		ND		ND	ND	ND		0.70600	6
FG FI ME 1	*Atractosteus messelensis*	Scale		SMF ME 11282	E8/9–18260	150–240 cm above α	9.3	0.0	−2.2	0.1	28.7	4.3	19.9	0.3	ND	
FK FI ME 2a	*Cyclurus kehreri*	Bone	Rib	SMF ME 11281	E8/9–25617	250–350 cm above α	10.1	0.1	−1.6	0.1	29.2	3.7	20.7	0.1	ND	
FG FI ME 2b	*Cyclurus kehreri*	Scale		SMF ME 11281	E8/9–25617	250–350 cm above α	10.8	0.1	−1.6	0.1	29.2	4.2	21.0	0.1	ND	
FK FI ME 3a	*Amphiperca multiformis*	Bone	Vertebrae	SMF ME 11283	E8/9–24730	250–350 cm above α	8.6	0.2	−1.2	0.2	29.6	3.8	20.2	0.1	ND	
FK FI ME 3b	*Amphiperca multiformis*	Bone	Rib	SMF ME 11283	E8/9–24730	250–350 cm above α	9.1	0.1	−1.5	0.1	29.4	4.7	20.1	0.2	ND	
FG FI ME 14-913	*Cyclurus kehreri*	Scale		No nr. (field sample)	i14–913	95–175 cm above M	8.0	0.1	−1.5	0.1	29.3	4.8	19.3	0.2	0.70633	10
FK FI ME 14-913	*Cyclurus kehreri*	Bone		No nr. (field sample)	i14–913	95–175 cm above M	7.9	0.1	−1.7	0.1	29.2	5.0	19.3	0.3	ND	
FK FI ME 14-966	*Cyclurus kehreri*	Bone		No nr. (field sample)	i14–966	95–175 cm above M	6.1	0.1	−3.6	0.1	27.2	4.2	19.1	0.4	0.70592	37
FG FI ME 14-966	*Cyclurus kehreri*	Scale		No nr. (field sample)	i14–966	95–175 cm above M	6.1	0.1	−2.9	0.1	27.9	3.9	19.3	0.3	ND	
FK FI ME 14-1063	*Atractosteus messelensis*	Bone		No nr. (field sample)	i14–1063	95–175 cm above M	8.4	0.1	−3.8	0.1	27.0	2.9	19.8	0.2	ND	
FG FI ME 14-1063	*Atractosteus messelensis*	Scale		No nr. (field sample)	i14–1063	95–175 cm above M	6.7	0.1	−3.4	0.1	27.4	2.8	19.5	0.3	0.70515	41
FK SCH ME 1	*Allaeochelys crassesculpta*	Bone	Dermal plate	SMF ME 11285	E8/9–26636	250–350 cm above α	7.3	0.1	−3.1	0.1	27.7	6.2	21.6	0.1	0.70552	6
FK SCH ME 2	Turtle indet?	Bone	Dermal plate	SMF ME 11375	E8/9–29234	350 cm above α	7.6	0.0	−3.9	0.1	26.9	8.7	23.7	0.1	0.70579	4
FD KR ME 1	*Diplocynodon darwini*	Dentine		SMF ME 11284	E8/9–24487	419 cm above α	ND		ND		ND	ND	22.2	0.2	0.70405	5
FZ KR ME 1	*Diplocynodon darwini*	Enamel		SMF ME 11284	E8/9–24487	419 cm above α	ND		ND		ND	ND	20.9	0.4	ND	
FK KR ME 1	*Diplocynodon darwini*	Bone		SMF ME 11284	E8/9–24487	419 cm above α	3.6	0.0	−3.7	0.0	27.1	8.2	21.4	0.4	0.70467	9
FK KR ME 1a	*Diplocynodon darwini*	Bone	Long bone	SMF ME 11285	E8/9–24487	419 cm above α	1.1	0.2	−2.4	0.1	28.4	6.7	20.0	0.2	0.70641	4
FK KR ME 1b	*Diplocynodon darwini*	Bone	Dermal plate	SMF ME 11286	E8/9–24487	419 cm above α	4.1	0.1	−2.9	0.1	28.0	6.8	20.8	0.1	0.70450	24
FK KR ME 2	Crocodile indet.	Bone		SMF ME 11553	E8/9–29226	350–450 cm above α	11.3	0.1	−1.5	0.1	29.4	10.8	22.6	0.1	0.70717	5
ME COP 1	Crocodile indet.	Coprolite		No nr. (field sample)	ND	ND	14.3	0.1	−2.3	0.1	28.6	12.1	20.3	0.2	0.70709	9
ME COP 2	Indet.	Coprolite		No nr. (field sample)	ND	ND	10.9	0.1	−2.3	0.1	28.6	6.5	ND		ND	
ME COP 3	Indet.	Coprolite		No nr. (field sample)	ND	ND	10.0	0.1	−2.4	0.1	28.5	5.8	19.0	0.1	ND	
ME COP 4	Indet.	Coprolite		KOE no nr.	ND	ND	ND		ND		ND	ND	20.7	0.1	ND	
ME COP 4/2011-4	Indet.	Coprolite		No nr. (field sample)	i14	95–175 cm above M	ND		ND		ND	ND	18.9	0.2	ND	
ME COP 4/2011-3	Indet.	Coprolite		No nr. (field sample)	i14	95–175 cm above M	ND		ND		ND	ND	20.0	0.2	ND	
ME COP 4/2011-1	Indet.	Coprolite		No nr. (field sample)	i14	95–175 cm above M	ND		ND		ND	ND	20.5	0.6	ND	
ME COP 4/2011-7	Indet.	Coprolite		No nr. (field sample)	i14	95–175 cm above M	ND		ND		ND	ND	21.1	0.4	ND	
ME COP 4/2011-9	Indet.	Coprolite		No nr. (field sample)	i14	95–175 cm above M	ND		ND		ND	ND	19.8	0.7	ND	

Table 3
Isotope (C, O, Sr) compositions of oil shale and authigenic minerals.

Sample-nr.	Material	Specimen-nr.	Excavation site–find-nr.	Stratigraphic level	$\delta^{13}C$ (‰ VPDB)	SD	$\delta^{18}O_{CO_3}$ (‰ VPDB)	SD	$\delta^{18}O_{CO_3}$ (‰ VSMOW)	$\%CO_3$	$\delta^{18}O_{PO_4}$ (‰ VSMOW)	SD	$^{87}Sr/^{86}Sr$	SD (ppm)
SED ME 1	Oil shale	SMF-ME 11284	E8/9–24487	419 cm above α	14.8	0.1	0.3	0.1	31.2	4.7	ND		0.70625	7
SED ME 2	Siderite	SMF-ME 11284	E8/9–24488	419 cm above α	17.8	0.1	1.5	0.0	32.4	51.0	ND		0.70461	4
SED FK SCH ME 2	Siderite	SMF-ME 11375	E8/9–29234	350 cm above α	17.5	0.0	2.7	0.0	33.7		ND		0.70556	11
SED FK KR ME 2	Siderite	SMF-ME 11553	E8/9–29226	350–450 cm above α	17.7	0.0	2.2	0.1	33.1		ND		ND	
Min ME 3	Montgomeryite			Marker bed M	ND		ND		ND		21.3	0.1	0.70673	6
Min ME 1	Messelite			Double messelite layer	ND		ND		ND		20.9	0.3	ND	
Min ME 2	Messelite			ND	ND		ND		ND		18.6	0.4	0.70558	10

methods has, however, now yielded a value of 21.7‰ and will hopefully lead to an unambiguous consensus value.

4.5. Strontium isotope analysis

Three hundred milligrams of dried wood was ashed at 500 °C for 3 h in porcelain crucibles. 10 mg of wood ash was dissolved in 1 ml distilled concentrated HNO_3 in Savillex beakers on a hotplate at 130 °C over night. About 2–3 mg pretreated bioapatite powder was digested as per the ash samples. Rock powders (i.e., oil shales) were ashed at 550 °C for 3 h to remove organics and 30 mg digested in a mixture of 3 ml HF and 1 ml HNO_3. After evaporation to dryness all samples were dissolved in 0.3 ml of 0.14 M HNO_3 and loaded after centrifugation on pre-cleaned Evergreen Scientific 0.5 ml mini-columns with 45–90 μm filters filled with 300 μl of Eichrom Sr-Spec resin (mesh 50–100 μm) for the Sr separation. Strontium was eluted in 1 ml 0.01 M HNO_3. Aliquots of the sample solution (10 μl diluted with 990 μl 0.14 M HNO_3) were measured using a Neptune MC–ICP-MS to determine the Sr content in the sample solution via the intensity of the ^{88}Sr signal compared to that of a 100 ppb Sr solution. The sample solutions were diluted to obtain a signal intensity of about ≥3 V on mass ^{88}Sr for the Sr isotope measurement. The NBS 987 standard and sample solutions were run at the same intensities using a ThermoFinnigan Neptune MC–ICP-MS at the University of Bonn. For sample introduction an Elemental Scientific SC-2 DX autosampler was used connected via a PFA 100 μl nebulizer to a 40 ml Scott-type borosilicate glass spray chamber. Strontium isotope ratios were measured in three blocks of 20 scans each and a washout time of 10 min in between samples. Measured $^{87}Sr/^{86}Sr$ values were corrected for mass bias using the exponential law and interferences. ^{85}Rb was monitored and used for correction of ^{87}Rb using the natural $^{87}Rb/^{85}Rb$ of 2.59265. Only measurements with an $^{85}Rb/^{86}Sr$ of <0.001 were accepted. ^{83}Kr was monitored and was <0.002 V for all measurements. Mass bias and interference corrected $^{87}Sr/^{86}Sr$ measurements were normalised to the accepted value of 0.71025 for the NBS 987 standard on a daily basis. In each measurement session after 3 samples one NBS 987 was measured for quality control and to monitor for any drift in isotope ratios. External precision (2 RSD) of $^{87}Sr/^{86}Sr$ measurements was better than 0.00003. Total procedure blanks were typically <200 pg for Sr.

5. Results

5.1. Carbon isotopic composition of vertebrate fossils

Carbon isotope compositions ($\delta^{13}C$) of the different bioapatite samples (n = 28, Table 2) cover a large range of about 20‰, from −9.8‰ in the enamel of the terrestrial hippomorph *Propalaeotherium* up to +11.3‰ in the bone of the crocodile *Diplocynodon*. The $\delta^{13}C$ values of the terrestrial and aquatic vertebrate remains cluster in distinct ranges (Fig. 2). While enamel of the hippomorph perissodactyl *Propalaeotherium* still has $\delta^{13}C$ values (~ −10 to −8‰, n = 6) expected for a C_3 plant feeder, the dentine samples from two of these teeth have $\delta^{13}C$ values of +5.6 and +8.7‰, far more positive than that expected for even C_4 plant feeders (Fig. 2).

All bones and scales of the aquatic vertebrates have positive $\delta^{13}C$ values (1.1‰ to 10.8‰) that are much higher than those of the enamel of *Propalaeotherium*. The crocodile (FK KR ME 1) has bone $\delta^{13}C$ values of 1.1‰ to 4.1‰ (n = 3), while the carbonate from embedding oil shale has a $\delta^{13}C$ value of 14.8‰. The siderite from the encrustation of this crocodile has an even higher value of 17.8‰ (Fig. 2). Scales and bones of the three analysed fish taxa *Atractosteus*, *Amphiperca* and *Cyclurus* have even higher $\delta^{13}C$ values than the crocodile ranging from 6.1 to 10.8‰ (n = 11). Intra-individual $\delta^{13}C$ differences between scale and bone samples from the same fish are ≤0.7‰, except for one *Atractosteus* specimen with a larger difference of 1.7‰ (Fig. 2). The two turtle bones have similar $\delta^{13}C$ values (7.3‰ and 7.6‰) to the fish remains. Phosphatised coprolites have the highest bioapatite $\delta^{13}C$ values of 10 to 14‰, with the most positive value occurring in a large crocodile coprolite (Fig. 2). Siderite crusts around vertebrate fossils (one turtle and one crocodile) have $\delta^{13}C$ values (17.7‰ and 17.8‰), which are the highest siderite values measured so far in Messel (Fig. 2, Table 3).

5.2. Oxygen isotopes ($\delta^{18}O_p$, $\delta^{18}O_c$) of vertebrate fossils

The phosphate oxygen isotope composition ($\delta^{18}O_p$) of vertebrate fossils from Messel range from 17.6‰ to 23.7‰ (n = 35; Table 2). The enamel of the terrestrial hippomorph *Propalaeotherium* has the lowest $\delta^{18}O_p$ of 18.1 ± 0.6‰ (range: 17.6‰ to 19.0‰, n = 6), while dentine of two teeth has somewhat higher values of 18.3‰ and 20‰. Bones and scales of the three fish taxa *Atractosteus*, *Amphiperca* and *Cyclurus* have $\delta^{18}O_p$ values of 19.9 ± 0.6‰ (range: 19.1‰ to 21.0‰; n = 11), which are, on average, about 2‰ higher than those of *Propalaeotherium* teeth. Phosphatic coprolites, presumably of fish and a crocodile (ME COP 1), have $\delta^{18}O_p$ values of 18.9‰ to 21.1‰ (n = 8), similar to those of the fish remains. The highest $\delta^{18}O_p$ values were measured for bones of two aquatic turtles (*Allaeochelys*: 21.6‰ and 23.7‰) and crocodiles (*Diplocynodon*: 20.0‰ to 22.6‰, n = 5, including one tooth).

Bioapatite carbonate $\delta^{18}O_c$ values of the same specimens range from 24.6‰ to 29.6‰ (n = 28; Table 2). Except for two turtle and crocodile bones the bioapatite samples have a $\Delta(\delta^{18}O_c–\delta^{18}O_p)$ offset between 7‰ and 10‰ and fall well in the $\delta^{18}O_c–\delta^{18}O_p$ equilibrium array for modern mammals (Iacumin et al., 1996; Pellegrini et al., 2011; Fig. 4). This indicates a good preservation of original $\delta^{18}O$ values in these specimens. Hence $\delta^{18}O_p$ values of *Propalaeotherium* enamel can be used to determine the $\delta^{18}O_{H_2O}$ value of their drinking water. Bone $\delta^{18}O_p$ values of aquatic turtles and crocodiles are used to estimate the lake water $\delta^{18}O_{H_2O}$ using according transfer functions from the literature. This value is then taken to calculate water temperatures using a fish

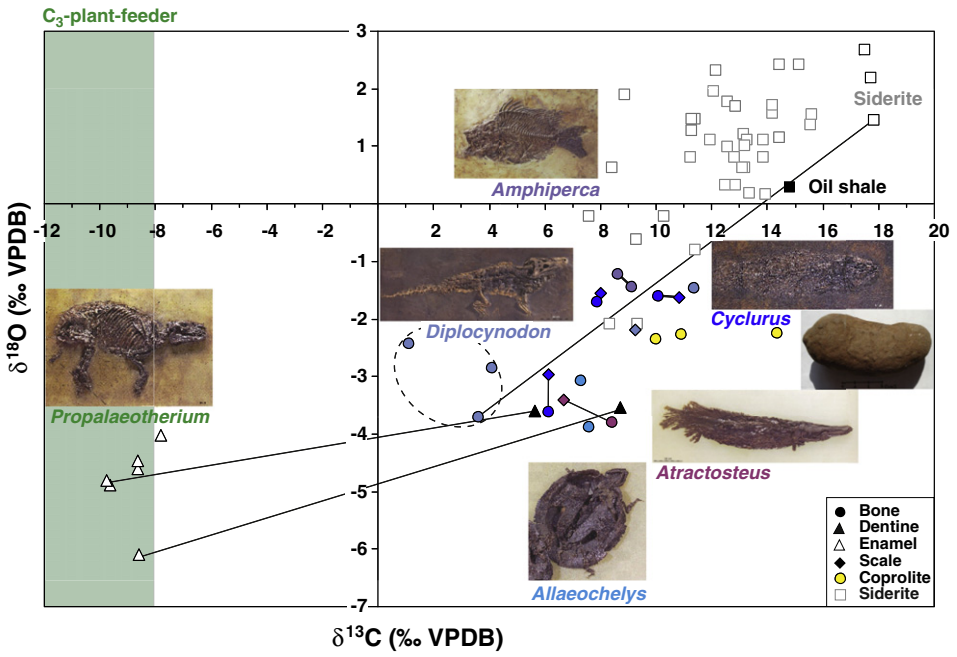

Fig. 2. Carbon and oxygen isotope composition of the carbonate in biogenic apatite of vertebrate fossils from Messel (Table 1): teeth of the terrestrial hippomorph *Propalaeotherium* (enamel, dentine), bones and scales of three fish taxa *Atractosteus*, *Amphiperca* and *Cyclurus* as well as bones of the aquatic turtle *Allaeochelys* and the crocodile *Diplocynodon*. Photographs of vertebrate fossils are taken from Gruber and Micklich (2007). Samples from the same individual are connected with a solid line. Siderite ($FeCO_3$) data from the Messel oil shale are from Bahrig (1989) and Felder and Gaupp (2006); except for three siderite crusts from vertebrate fossils (black open quadrates). Note that enamel of *Propalaeotherium* still has low $\delta^{13}C$ values typical for a C_3 plant feeder, while dentine of the same teeth is shifted >15‰ towards diagenetic end member values of ^{13}C-rich siderite.

bone/scale and coprolite $\delta^{18}O_p$ values using a revised phosphate–water oxygen isotope equilibrium fractionation equation (Lécuyer et al., 2013; Table 1).

5.3. Strontium isotopes ($^{87}Sr/^{86}Sr$) of rocks, wood and vertebrate fossils

The $^{87}Sr/^{86}Sr$ of rock samples from the Messel FB 2001 drill core and five other drill cores cover a broad range from 0.70365 to 0.72287 (n = 18, Table 3). The lowest value was measured in the basalt fragment from the lapilli tuff infill of the diatreme below the Messel maar oil shale, which was Ar–Ar dated to 47.8 Ma by Mertz and Renne (2005) and the highest value in an Upper Permian (Rotliegend) conglomerate sample from exploration well TB2 (Fig. 3; Table 3). Oil shale samples have low $^{87}Sr/^{86}Sr$ <0.707 (0.70491 to 0.70665, n = 5) only a siderite sample has a slightly lower value of 0.70461. The authigenic phosphate minerals messelite and montgomeryite have $^{87}Sr/^{86}Sr$ of 0.70558 and

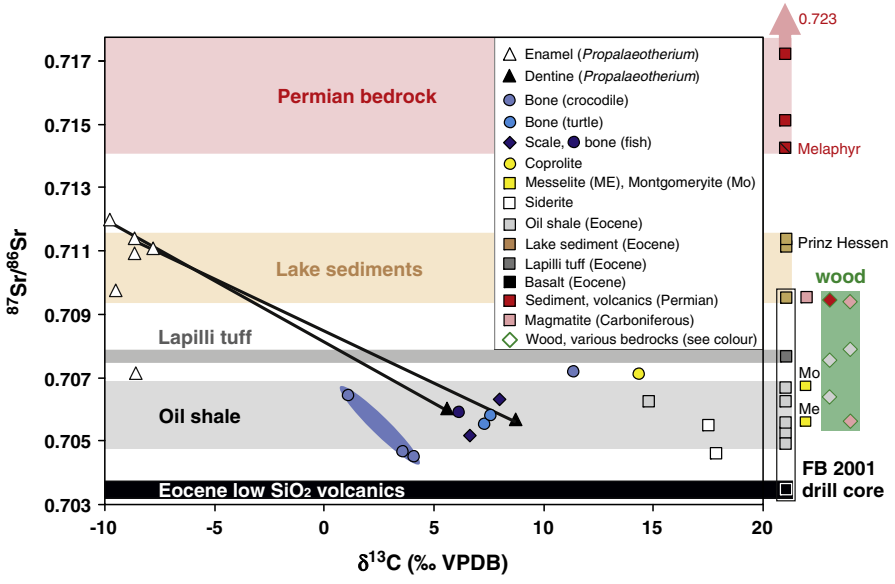

Fig. 3. Strontium ($^{87}Sr/^{86}Sr$) and carbon ($\delta^{13}C$) isotope compositions of rocks, minerals, wood and phosphatic fossils from the Messel Pit (Tables 2 to 5). The Permian rocks come from different drill cores (FB GA 1, GA 2, TB 2) in the vicinity of Messel. Oil shale, lapilli tuff and siliciclastic lake sediments are from the Messel FB 2001 research drill core (Felder and Harms, 2004), except for two siliciclastic lake sediments from the Grube Prinz von Hessen. The range of $^{87}Sr/^{86}Sr$ values of Eocene low SiO_2 volcanic rocks are drawn after data from Dieter Mertz (pers. comm. 2014). Wood samples were collected on different bedrock substrates (colour infill matches to the according bedrock substrate) in the Messel Pit (Table 5). Enamel and dentine samples from the same *Propalaeotherium* teeth are connected by solid lines.

Table 4
Strontium isotope composition of rocks from drill cores of the Messel area.

Sample-nr.	Material	Locality	Drill core (depth) or provenance	Age	$^{87}Sr/^{86}Sr$
2011-241	Silt-sand	Prinz Hessen, 3.3 km SW Messel Pit	Prinz Hessen (85.5 m)	Middle Eocene	0.71114
2011-242	Silt-sand	Prinz Hessen, 3.3 km SW Messel Pit	Prinz Hessen (68 m)	Middle Eocene	0.71137
2011-339	Oil shale	Messel Pit	IN 25 (6 m)	Middle Eocene	0.70779
Min ME 3	Montgomeryite	Messel Pit	Messel (3.8 m; marker horizon M)	Middle Eocene	0.70673
SED ME 1	Oil shale	Messel Pit, NW slope E8/9	Excavation 2007, SMF-ME 11284 (23.16 m)	Middle Eocene	0.70625
SED ME 2	Siderite	Messel Pit, NW slope E8/9	Excavation 2007, SMF-ME 11284 (23.16 m)	Middle Eocene	0.70461
SED SCH ME 2	Oil shale	Messel Pit, NW slope E8/9	Excavation 2008, SMF-ME 11375 (23.85 m)	Middle Eocene	0.70556
2011-231	Oil shale	Messel Pit, center	FB 2001 Messel (5 m)	Middle Eocene	0.70524
2011-232	Oil shale	Messel Pit, center	FB 2001 Messel (57 m)	Middle Eocene	0.70665
2011-233	Silt-sand	Messel Pit, center	FB 2001 Messel (103 m)	Middle Eocene	0.70952
2011-234	Oil shale	Messel Pit, center	FB 2001 Messel (123 m)	Middle Eocene	0.70491
BA ME 1	Basalt	Messel Pit, center	FB 2001 Messel (268 m)	Middle Eocene	0.70365
2011-235	Lapilli tuff	Messel Pit, center	FB 2001 Messel (285 m)	Middle Eocene	0.70766
2011-236	Lapilli tuff	Messel Pit, center	FB 2001 Messel (351 m)	Middle Eocene	0.70438
2011-223	Mudstone	2.6 km SW of Messel Pit center	FB Messel GA 1 (11 m)	Upper Permian (Rotliegend)	0.71718
2011-224	Melaphyr	2.6 km SW of Messel Pit center	FB Messel GA 1 (19–20 m)	Upper Permian (Rotliegend)	0.71425
2011-230	Sandstone	2 km SW of Messel Pit center	FB Messel GA 2 (7–8 m)	Upper Permian (Rotliegend)	0.71511
2011-228	Mudstone	2 km SW of Messel Pit center	FB Messel GA 2 (5.5 m)	Upper Permian (Rotliegend)	0.72188
2011-220	Granitoid	0.5 km E of Messel Pit center	TB 2 (68 m)	Upper Permian (Rotliegend)	0.70953
2011-219	Sandstone	0.5 km E of Messel Pit center	TB 2 (12 m)	Upper Permian (Rotliegend)	0.72287
Min ME 2	Messelite	Messel Pit	Double messelite marker bed (18 m)	Middle Eocene	0.70558
H_2O ME 1	Groundwater	Messel Pit, center	FB 2001 drill hole (well)	Recent	0.70860

0.70673, respectively, similar to oil shale values (Fig. 3) indicating the influence of unradiogenic Sr from mantle-derived volcanic rocks on the lake water.

In contrast, Upper Permian sedimentary and volcanic rocks have the highest $^{87}Sr/^{86}Sr$ values >0.714 (Rotliegend mudstones and conglomerates: 0.71511 to 0.72287 (n = 4); one intermediate volcanic rock "melaphyr": 0.71425; Table 3, Fig. 3). Wood samples from modern trees growing on Eocene oil shale and Carboniferous/Permian bedrock (granite, diorite) in the Messel pit reflect bioavailable $^{87}Sr/^{86}Sr$ values ranging only from 0.70562 to 0.7094 (n = 6, Table 5). The two wood samples from Eocene oil shale (0.70638 to 0.70756) plot at the upper range of oil shale values (Fig. 3). The single wood sample from a tree that grew on presumable Permian sedimentary rock has a significantly lower $^{87}Sr/^{86}Sr$ of 0.7094 compared to Permian siliciclastic rocks (0.715 to 0.723) from drill core samples (Fig. 3).

Bioapatite $^{87}Sr/^{86}Sr$ values range from 0.70405 to 0.71199 (n = 17, Table 3). There is a clear bimodal distribution of bioapatite $^{87}Sr/^{86}Sr$ values. Aquatic vertebrates have low $^{87}Sr/^{86}Sr \leq 0.707$ similar to the embedding oil shale (Fig. 3). The lowest values were measured in bone and tooth samples of a crocodile *Diplocynodon* (0.70405 to 0.70641, n = 3) and bones of two *Allaeochelys* turtles (0.70552 to 0.70557, n = 2). A coprolite from a crocodile (ME COP 1) and the bone of a second crocodile have the highest $^{87}Sr/^{86}Sr$ (both around 0.7071) of all aquatic vertebrate samples. In contrast, most enamel samples of *Propalaeotherium* have much more radiogenic $^{87}Sr/^{86}Sr$ of ~0.711 (0.71093 to 0.71199, n = 4, Table 2) except for two samples with 0.70713 and 0.70972, which are above oil shale values but close to a lapilli tuff sample (Fig. 3). Dentine samples from two of these teeth with $^{87}Sr/^{86}Sr$ of ~0.711 have much lower $^{87}Sr/^{86}Sr$ of 0.70567 and 0.70598 that fall in the range of oil shales and authigenic phosphates (Table 3, Fig. 3). The same applies to the bone of the terrestrial arboreal mammal *Kopidodon* with a value of 0.706.

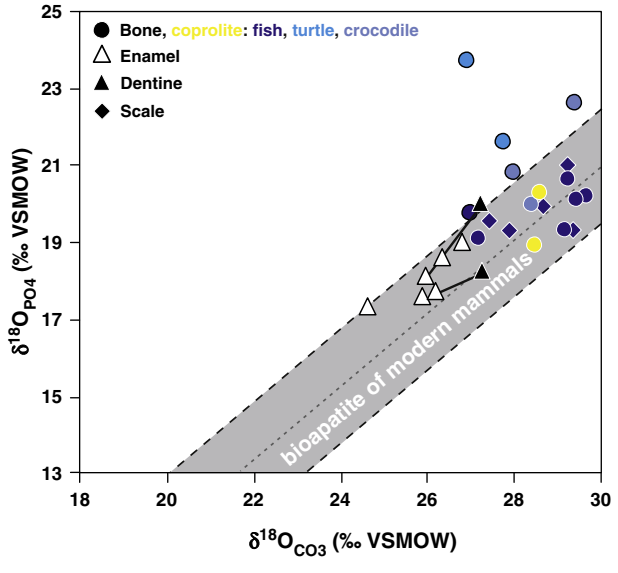

Fig. 4. Oxygen isotope composition of the carbonate ($\delta^{18}O_{CO_3}$) and phosphate ($\delta^{18}O_p$) of the bones, teeth, scales and coprolites from Messel. Except for a few turtle and crocodile bones all samples fall in the isotope equilibrium $\Delta(\delta^{18}O_{CO3}-\delta^{18}O_p)$ array of bones and teeth of modern mammals drawn after Pellegrini et al. (2011). Note, however, that $\delta^{18}O$ values of the dentine from the two *Propalaeotherium* teeth are shifted towards higher values, likely due to some diagenetic alteration.

6. Discussion

6.1. Carbon isotopes: preservation in enamel — alteration of dentine and bone

The setting of Messel offers a unique possibility to trace diagenetic alteration of bioapatite carbon isotope signatures. In Messel the diagenetic $\delta^{13}C$ value is isotopically so distinct from that of a C_3 browser that any major alteration would have resulted in a very pronounced shift towards positive $\delta^{13}C$ values (as observed for the dentine). The ^{13}C-enrichment in the bioapatite and siderite reflects the dissolved

Table 5
Sr isotope composition of extant wood samples from the Messel pit.

Sample	Material	Taxon	Bedrock, age	$^{87}Sr/^{86}Sr$	SD (ppm)
W ME 1	Wood	*Fagus silvatica*	Diorite, Carboniferous	0.705615	4
W ME 2	Wood	*Quercus robur*	Oil shale, M Eocene	0.707556	18
W ME 3	Wood	*Betula pendula*	Granite, Carboniferous	0.709398	18
W ME 4	Wood	*Quercus robur*	Oil shale, M Eocene	0.706375	13
W ME 5	Wood	*Fagus silvatica*	Sediment, U Permian	0.709390	6
W ME 6	Wood	*Fagus silvatica*	Diorite, Carboniferous	0.707874	11

inorganic carbon (DIC) of the lake water. Due to permanent anoxic conditions in the bottom water of the stratified, meromictic Messel lake low Eh conditions led to methanogenesis and the formation of siderite, which is typical for meromictic longterm lakes (Bahrig, 1989; Felder and Gaupp, 2006). High $\delta^{13}C$ values of the siderite result from the degassing of ^{12}C-rich methane leading to a ^{13}C-enrichment in the remaining DIC (Felder and Gaupp, 2006), which is reflected in the positive $\delta^{13}C$ values of the authigenic siderite (Fig. 2). Thus positive $\delta^{13}C$ signatures can be used to monitor for diagenetic alteration in vertebrate bioapatite.

6.1.1. Preservation of near-in vivo $\delta^{13}C$ values in enamel of Propalaeotherium

Enamel samples of the brachydont hippomorph perissodactyl *Propalaeotherium hassiacum* still have low enamel $\delta^{13}C$ values around −9‰, typical for a C_3 plant feeder, albeit at the upper end of the $\delta^{13}C$ range (Fig. 2). This is well in accordance with gut contents of *Eurohippus parvulus* and *Propalaeotherium hassiacum* indicating a foliage-dominated diet (Sturm, 1978; Richter, 1987) with addition of fruits (i.e. grapes) (von Koenigswald and Schaarschmidt, 1983; Franzen, 1995, 2007). These were ingested by foraging in a paratropical forest canopy (Wilde, 1989, 2004; Collinson et al., 2012) of a C_3 plant ecosystem. Based on gut contents of *Propalaeotherium isselanum* from slightly younger middle Eocene deposits (MP 13) of the Geiseltal, opportunistic folivorous feeding habits that also included flowers and fruits/seeds (Wilde and Hellmund, 2010) can be inferred for *Propalaeotherium*.

Using *Propalaeotherium* enamel $\delta^{13}C$ values (−9.8‰ to −7.8‰) and assuming the $\varepsilon_{diet-enamel}$ fractionation factor of +14‰ for extant ungulates (although non-ruminants may have a smaller isotope enrichment between 12‰ to 13‰; Cerling and Harris, 1999) is also valid for *Propalaeotherium*, $\delta^{13}C$ values between −23.8‰ and −21.8‰ can be calculated for the ingested food plants. These values are at the upper end of the range of extant C_3 plants (−36‰ to −22‰, Farquhar et al., 1989) and also 1.5‰ to 6.6‰ higher than $\delta^{13}C$ values of plant fossils from Messel such as cuticles of fossil leaves of Myrtaceae and Lauraceae (−28.4 ±1.1‰; Grein et al., 2010), other terrestrial plant leaves (−26.8 ±0.8‰), seeds (25.8 ± 1.2‰) and palm fruits (−25.3 ± 0.5‰) (Schweizer et al., 2007). Thus lower $\delta^{13}C$ values below -14‰ are to be expected for the enamel of a sub-canopy browser in such a subtropical forest setting. Several possibilities can account for elevated enamel $\delta^{13}C$ values: (1) *Propalaeotherium* had ingested other, isotopically more ^{13}C-enriched food plants, (2) the $\varepsilon_{diet-enamel}$ fractionation factor for *Propalaeotherium* is >14‰ (e.g. because of methane loss during digestion; see Passey et al. (2005) for details) or (3) the enamel was affected by diagenesis in the ^{13}C-rich water of Lake Messel, which may have shifted $\delta^{13}C$ values to slightly more positive values. Such a diagenetic alteration becomes clearly apparent in the dentine samples of the same teeth, which have up to 17‰ higher $\delta^{13}C$ values of 5.6‰ and 8.6‰ (Fig. 2). The dentine values are even higher than $\delta^{13}C$ enamel values for mammalian C_4 plant feeders and this is the largest difference between these two dental tissues of a single tooth that has been reported so far. The strong ^{13}C-enrichment in the dentine is clearly due to a diagenetic alteration either by isotopic exchange and the addition of carbonate during transformation of hydroxyapatite into francolite (Lécuyer et al., 2003) and/or incorporation of authigenic ^{13}C-rich siderite (Bahrig, 1989; Felder and Gaupp, 2006) in pore space such as dental tubuli. The latter should ideally have been removed during acetic acid treatment. However, due to short pre-treatment times and the low solubility of siderite compared to other carbonates (Larson et al., 2008), siderite removal might not have been complete. Only few bone samples from the two crocodiles and one turtle have CO_3 contents higher than expected for modern bone and display high $\delta^{13}C$ values and CO_3 contents (Fig. 5). However, CO_3 contents of the dentine samples still fall in the expected 3–6 wt.% range of CO_3 for modern bones (Fig. 5). Thus siderite infillings in pore space such as dentine canals is probably not the cause for positive dentine $\delta^{13}C$ values. Either carbonate exchange with the lake water DIC and/or the addition of secondary apatite may have caused the high $\delta^{13}C$ values as the formation of authigenic phosphate minerals, such as messelite and montgomeryite, which are well-known (Felder, 2007). The *Propalaeotherium* enamel seems only affected by minor diagenetic alteration as $\delta^{13}C$ values are shifted only slightly towards the diagenetic end member values, indicating that no major exchange of enamel carbonate with the ^{13}C-rich DIC of the lake and/or pore water had occurred (Fig. 3). Overall the 47 Ma-old enamel of *Propalaeotherium* still preserves near-in vivo $\delta^{13}C$ values, while dentine is clearly altered.

6.1.2. Alteration of $\delta^{13}C$ values in bones and scales of aquatic vertebrates

All bones and scales of aquatic vertebrates (crocodile, turtle, fish) have 10–20‰ higher bioapatite $\delta^{13}C$ values in their skeletal remains then the enamel of the terrestrial *Propalaeotherium* (Fig. 2). For aquatic vertebrates that lived and fossilised in lake water with ^{13}C-rich DIC it is difficult to distinguish if the positive $\delta^{13}C$ values were incorporated in vivo or post mortem. However, as bone is even more prone to diagenetic alteration than dentine, a post mortem carbonate exchange with the ^{13}C-rich DIC from the lake water is very likely. The crocodile (FK KR ME 1) has the lowest bone $\delta^{13}C$ values (1 to 4‰) of all aquatic vertebrates while the embedding oil shale and the siderite crust around the fossil have >10‰ higher $\delta^{13}C$ values of 14.3 and 17.8‰, respectively. The diagenetic carbonate exchange of bone apatite with the lake/pore water did not completely homogenise $\delta^{13}C$ values which still might be – at least partially – preserved. The relatively low $\delta^{13}C$ values of the crocodile bones might still reflect that the semi-aquatic *Diplocynodon* partially fed on terrestrial vertebrates with low C_3 plant feeder-like $\delta^{13}C$ values. In contrast the fully aquatic vertebrates, such as the three fish taxa, that ingested food from the ^{13}C-rich lake water display somewhat higher $\delta^{13}C$ values (Fig. 2). These isotopic differences in $\delta^{13}C$ (as well as $\delta^{18}O$) values might still reflect some ecological differences between the aquatic vertebrates.

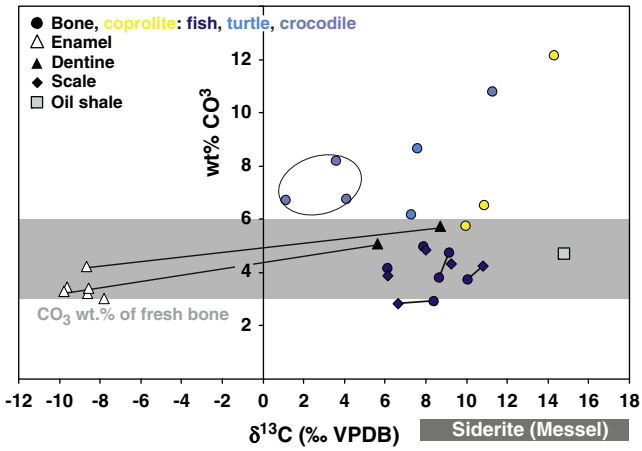

Fig. 5. Plot of $\delta^{13}C$ versus wt.% CO_3 of bone, tooth, scale and coprolite samples of Messel vertebrates. Most samples fall in the range of carbonate content of modern bones (3–6 wt.%; Pasteris et al., 2008), except for a few turtle and crocodile bones. The latter display high CO_3 contents and $\delta^{13}C$ values, which probably reflects incomplete removal of diagenetic ^{13}C-rich siderite by acid treatment. For the other samples treatment for carbonate removal seems to have been successful. For instance enamel samples still have low CO_3 contents and low $\delta^{13}C$ values. In contrast, dentine samples of the same teeth have >15‰ higher $\delta^{13}C$ values despite only slightly higher CO_3 contents. This hints towards a diagenetic CO_3 exchange in the bioapatite rather than remaining siderite. The same probably also applies to the fish bones and scales, that still have CO_3 contents in the range of modern bone. Siderite $\delta^{13}C$ data are from Bahrig (1989) and Felder and Gaupp (2006).

6.2. Oxygen isotopes: preservation of $\delta^{18}O$ values and temperature reconstructions

6.2.1. Preservation of original $\delta^{18}O$ values

Bioapatite oxygen isotope compositions $\delta^{18}O_p$ and $\delta^{18}O_c$" do not evidence substantial diagenetic alteration as samples plot within the array expected for bioapatite of modern vertebrates (Pellegrini et al., 2011; Fig. 4). Enamel values of *Propalaeotherium* notably the least affected by diagenesis, while dentine from two teeth are slightly shifted (0.5 to 1.9‰) towards higher $\delta^{18}O$ values. The dentine samples plot with fish bones and scales as well as coprolites, which phosphatised at the sediment–water interface in the bottom water hypolimnion of Lake Messel, thus reflecting predominantly diagenetic phosphate (Fig. 4). The oxygen isotope composition of enamel from the terrestrial *Propalaeotherium* is about 2–3‰ lower than those of bones and scales of aquatic vertebrates from the ^{18}O-enriched water of the Messel lake (Figs. 2, 4). For instance there is a 2.8‰ difference in enamel $\delta^{18}O_p$ values of *Propalaeotherium* and the crocodile *Diplocynodon*. Thus the use of isotopically-distinct water sources of terrestrial and aquatic vertebrates is still reflected in bioapatite $\delta^{18}O$ values.

The good preservation of enamel $\delta^{18}O_p$ values in Messel is further supported by triple oxygen (^{16}O, ^{17}O, ^{18}O) isotope analysis of a rodent tooth of *Masillamys* sp. (Gehler et al., 2011). In the enamel a negative $\Delta^{17}O$ anomaly (derived from inhaled air oxygen) of -0.18 ± 0.06‰ was found while this anomaly was nearly completely erased in the dentine of the same tooth (Gehler et al., 2011). Because the rare ^{17}O isotope is easily altered during diagenesis with a high fluid–apatite ratio the presence of a negative $\Delta^{17}O$ anomaly in enamel is a direct and sensitive indicator for the good preservation of the phosphate oxygen isotope composition (Gehler et al., 2011). If a negative $\Delta^{17}O$ anomaly is still preserved in such a small rodent tooth with thin enamel for the thicker enamel of larger *Propalaeotherium* teeth preservation of original $\delta^{18}O_p$ values is likely. Finally, the lack of bacterial activity in the anoxic bottom water of Lake Messel makes diagenetic alteration by microbial attack unlikely, which is known to affect enamel $\delta^{18}O_p$ values (Zazzo et al., 2004).

6.2.2. Reconstruction of drinking and lake water $\delta^{18}O_{H_2O}$ values

Phosphate oxygen isotope composition ($\delta^{18}O_p = 18.1 \pm 0.6$‰) of the well-preserved enamel of *Propalaeotherium* teeth can thus be used to calculate drinking water values (assumed to reflect meteoric water i.e. precipitation) for palaeoclimatic reconstruction. Using the species-specific relation between $\delta^{18}O_p$–$\delta^{18}O_{H_2O}$ for modern horses (Delgado Huertas et al., 1995; Table 1: Eq. (4)) a predicted drinking water $\delta^{18}O_{H_2O}$ value of -6.3 ± 0.9‰ can be reconstructed for the *Propalaeotherium*. The same value (-6.3 ± 0.7‰) was obtained using an all-mammal regression (Amiot et al., 2004; Table 1: Eq. (5)). *Propalaeotherium* was a predominant leaf browser with occasional addition of some fruits with a much smaller body mass (Franzen, 2007) than extant horses, which are grazers, thus it possibly had a different water-use strategy and metabolism than modern *Equus*. A significant part of its body fluid may have derived from ingested leaf water, which is usually strongly enriched in ^{18}O compared to surface water due to evapotranspiration (Yakir, 1997). However, as *Propalaeotherium* lived as a subcanopy browser (Franzen, 2007) in a humid paratropical rainforest the leaf water may not be strongly ^{18}O-enriched because less evapotranspiration occurred. For extant horses, which are obligate drinkers and have high water requirements for hindgut fermentation, the influence of relative humidity was found to be only of minor importance and can be assumed with 0.1‰/% relative humidity, which is a minimum assumption (Kohn and Fremd, 2007). Modern equid specimens used for the horse-specific $\delta^{18}O_p$–$\delta^{18}O_{H_2O}$ calibration originate from localities where the relative humidity clusters around 60% (pers. comm. M.J. Kohn 2014) while for Messel it was higher around 75 ± 2% (Grein et al., 2011a). Therefore, an adjustment of about +1.5‰ for the mean $\delta^{18}O_p$ value of *Propalaeotherium* to 19.6‰ is necessary to correct for this 15% difference in relative humidity. Using this $\delta^{18}O_p$ value and the horse-specific equation (Table 1: Eq. (4)) a drinking water $\delta^{18}O_{H_2O}$ value of -4.2 ± 0.9‰ can be calculated, taking humidity into account. Uncertainties in inferred $\delta^{18}O_{H_2O}$ must be at least ±1‰ because the modern equid database shows at least that much scatter.

Taxa with differences in physiology and water turnover can have significant differences in their $\delta^{18}O$ values (e.g., Kohn, 1996; Kohn et al., 1996, Levin et al., 2006). Enamel of more terrestrial vertebrates needs to be analysed to determine whether *Propalaeotherium* has elevated $\delta^{18}O_p$ values compared to other sympatric herbivores. Therefore the enamel of the aforementioned well-preserved rodent tooth of *Masillamys* from Messel was used to obtain an independent estimate of the meteoric water $\delta^{18}O_{H_2O}$ value. The enamel has a $\delta^{18}O_p$ value of 18.1‰ (Gehler et al., 2011), which is identical to the mean value of *Propalaeotherium* enamel. From this value a $\delta^{18}O_{H_2O}$ value of −5‰ can be calculated using the $\delta^{18}O_p$–$\delta^{18}O_{H_2O}$ equation for rodents (Navarro et al., 2004; Table 1: Eq. (3)). This $\delta^{18}O_{H_2O}$ value is similar to the value estimated for *Propalaeotherium* and does not support a strong ^{18}O enrichment of the water ingested by *Propalaeotherium*. Thus overall mammalian drinking water values of around −4 to 5‰ are calculated for Messel using species-specific empirical equations. This estimate for middle Eocene meteoric water $\delta^{18}O_{H_2O}$ value is about 4 ± 0.5‰ higher than Holocene groundwater in the Messel research well, which has a value of −8.5‰ (Eccarius et al., 2005).

In this study, the reconstruction of a $\delta^{18}O_{H_2O}$ value for Lake Messel water was also attempted. For this purpose the $\delta^{18}O_p$ values of turtle bones (*Allaeochelys*) as well as several bones and a tooth of *Diplocynodon* crocodiles were used, utilising empirical $\delta^{18}O_p$–$\delta^{18}O_{H_2O}$ regressions for modern aquatic turtles (Barrick et al., 1999 recalculated to match a value of 21.7‰ for the NBS 120c standard after Pouech et al., 2014, Table 1: Eq. (1)) and crocodilians (Amiot et al., 2007, Table 1: Eq. (2)). However, this approach is only valid if original bioapatite $\delta^{18}O_p$ values are preserved in bone and dentine of these aquatic vertebrates. Water $\delta^{18}O_{H_2O}$ values inferred from two turtle bones (0.3 and 1.7‰) are ^{18}O-enriched compared to crocodile bones of two individuals and one tooth that yield lower values (range: −0.5 to −2.7‰). The dentine of the crocodile tooth had a 1.4‰ higher $\delta^{18}O_p$ value than the enamel (Table 2), which records a $\delta^{18}O_{H_2O}$ value of −2‰. A similar pattern with dentine being enriched in ^{18}O compared to enamel from the same tooth by 0.5 to 1.9‰ is also observed for two *Propalaeotherium* teeth (Table 2). This indicates that dentine and thus likely also bone $\delta^{18}O_p$ values of Messel vertebrates were affected by some diagenetic alteration and probably shifted towards higher values (considering enamel–dentine pairs; Fig. 3). Hence the reconstructed $\delta^{18}O_{H_2O}$ values represent presumably maximum estimates of the Messel lake water and might be biased towards the composition of diagenetic fluids. The −2‰ value derived from the crocodile enamel may most closely reflect the Messel Lake water value. Note, however, this is only a single specimen and more data are clearly needed to confirm this preliminary estimate. Compared to the drinking water values around −5‰ reconstructed for terrestrial mammals from empirical species-specific equations the water of Lake Messel was enriched in ^{18}O by about 3‰ (Fig. 2). This is not unexpected as the Lake Messel existed for more than 640 ka (Lenz et al., 2010) and long-term lakes often have ^{18}O-enriched water bodies (Kelts and Talbot, 1990; Talbot, 1990; Tütken et al., 2006). Furthermore, a significant increase in abundance of pinaceous pollen in the vertebrate bearing upper part of the middle Messel Formation indicates a climate shift towards drier conditions (Lenz et al., 2011). This may have resulted in a negative hydrological budget of the lake, at least temporally. The fish fauna implies that at some stages the lake was connected to a river network (Micklich, 2012). However, for how long such connection existed, which water volume did flow into the lake and if the inflowing water was ^{18}O-enriched compared to local precipitation is unknown.

6.2.3. Reconstruction of air and water temperatures

6.2.3.1. Air temperature of Messel. The drinking water $\delta^{18}O_{H_2O}$ value of −6.3‰ determined using the calibration for extant horses and corrected for relative humidity to −4.2‰ (see Section 6.2.2 for details) indicates that *Propalaeotherium* did not ingest its water predominantly from the Messel lake ($\delta^{18}O_{H_2O}$ ~ −2‰) but likely from less ^{18}O-enriched precipitation-fed surface water sources (Fig. 6). Assuming *Propalaeotherium* ingested surface water and records middle Eocene meteoric water values a reconstruction of mean annual air temperature (MAT) can be attempted, based on the modern day relationship between $\delta^{18}O_{H_2O}$-MAT (Amiot et al., 2004, Table 1: Eq. (7)). However, it is necessary to correct the reconstructed $\delta^{18}O_{H_2O}$ values by −1‰ for the ice volume (Tindall et al., 2010 and references therein) to account for the lack of polar ice caps in the middle Eocene. A MAT of 18.3 ± 2.5 °C was calculated from the ice volume corrected drinking water $\delta^{18}O_{H_2O}$ value of −5.2‰ (Fig. 6), derived from the *Propalaeotherium* enamel $\delta^{18}O_p$ value using a Monte Carlo approach for error estimation. A similar MAT of 16.7 ± 1.7 °C was calculated for *Masillamys* using its ice volume corrected drinking water $\delta^{18}O_{H_2O}$ value of −6.0‰. These reconstructed MAT values fall in the temperature range of 16.8 to 23.9 °C estimated for Messel based on fossil plant macro remains using a co-existence approach (CA) of extant plant taxa (Grein et al., 2011a). However, they are lower than the MAT of ~22 ± 3 °C for Messel (Grein et al., 2011a) and the MAT of 24 ± 1 °C for the lower Eocene of the Geiseltal site in central Germany (Mosbrugger et al., 2005), both reconstructed using the CA.

Various causes can explain lower temperature estimates. Diagenetic alteration of $\delta^{18}O_p$ values in enamel can be excluded given the preservation of near-in vivo isotope compositions. Furthermore, diagenesis in Messel leads to increased $\delta^{18}O_p$ values (as evidenced by dentine samples of *Propalaeotherium*; Fig. 4, Table 1) and thus would have resulted in warmer not cooler MAT estimates. The same would apply to the ingestion of ^{18}O-enriched leaf/fruit water from the folivore/frugivore diet of *Propalaeotherium*, arguing indirectly against enriched leaf water $\delta^{18}O_{H_2O}$ values and strong effects of relative humidity. Migration and use of water sources with low $\delta^{18}O$ values distinct from local precipitation such as rivers from high elevation areas could explain low MAT estimates. However, there is neither any indication for long distance migration of *Propalaeotherium* (see Section 6.3.2) nor that high mountain ranges were present in the hinterland of Messel. Thus *Propalaeotherium* likely ingested its water from local water sources. However, besides air temperature many other factors (e.g. moisture source, rainout effects, and relative humidity) can affect $\delta^{18}O_{H_2O}$ values of precipitation. This may complicate the reconstruction of air temperatures. Therefore a simple linear regression between $\delta^{18}O_{H_2O}$-MAT for modern precipitation may not yield appropriate estimates for the Eocene meteoric water of Messel, especially as the relation is much less well constrained for subtropical–tropical lower latitude settings (e.g. Dansgaard, 1964; Fricke and O'Neil, 1999). Messel was situated at a latitude of about 46°N in a humid subtropical to tropical climate (Grein et al., 2011a) about 400 km south from the palaeo-coastline of the North Sea (Kockel, 1988). In such climatic settings the amount effect during precipitation might be strong and can lead to a higher amount of ^{16}O in rain water during rainout then expected from the global temperature–$\delta^{18}O_{H_2O}$ relation (Rozanski et al., 1993; Fricke and O'Neil, 1999). This would lead to an underestimation of MAT. Therefore I took another approach to infer a MAT for Messel by checking for a modern analogue station for

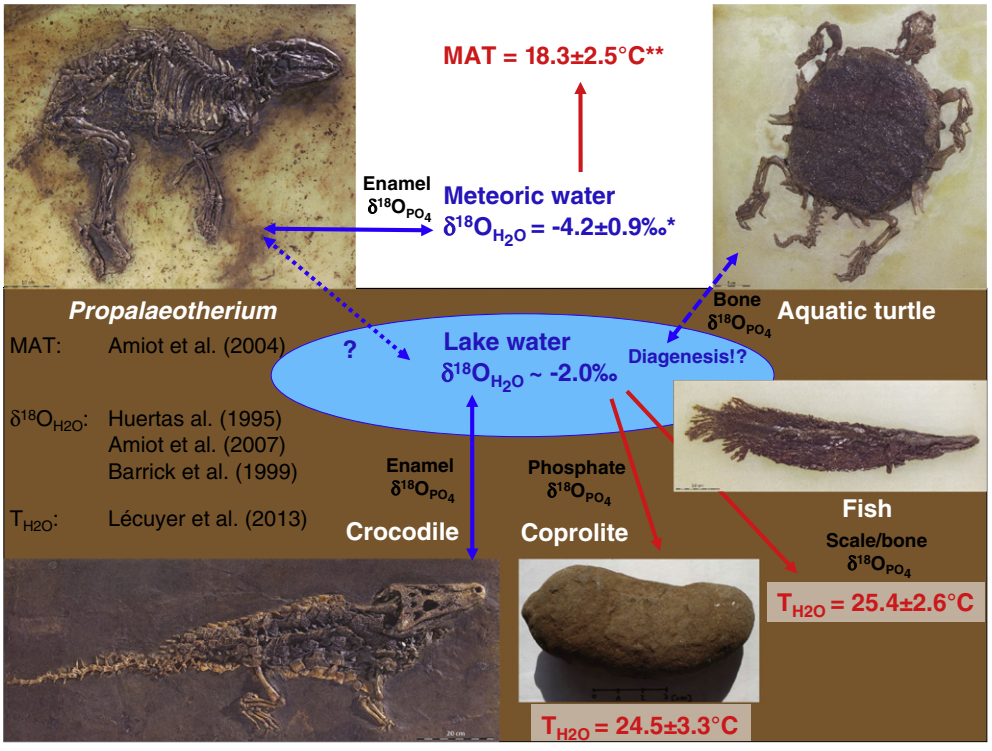

Fig. 6. Reconstructed air and water temperatures calculated from the $\delta^{18}O_p$ values of Messel vertebrate fossils using different transfer functions (Table 1). The drinking water $\delta^{18}O_{H_2O}$ value of the terrestrial hippomorph *Propalaeotherium* was reconstructed to −6.3‰ using both a horse specific (Delgado Huertas et al., 1995) as well as an all-mammal $\delta^{18}O_p$–$\delta^{18}O_{H_2O}$ regression (Amiot et al., 2004). Correcting for the effect of relative humidity (*) yields a $\delta^{18}O_{H_2O}$ value of −4.2‰ for the middle Eocene meteoric water. An additional correction of −1‰ for the difference in ice volume (**) between the Eocene and today (Tindall et al., 2010) needs to be applied prior to air temperature calculation. From this corrected value $\delta^{18}O_{H_2O}$ value of −5.2‰ a mean annual air temperature (MAT) of 18.3 ± 2.5 °C is determined using a modern-day MAT–$\delta^{18}O_{H_2O}$ relation (Amiot et al., 2004). A preliminary $\delta^{18}O_{H_2O}$ value for Lake Messel of about −2‰ was calculated from the enamel $\delta^{18}O_p$ value of a crocodile tooth using a taxon-specific transfer function for crocodilians (Amiot et al., 2007). Note, turtle bones yielded positive $\delta^{18}O_{H_2O}$ values of +0.3 and +1.7‰ using the recalculated Barrick et al. (1999) regression for aquatic turtles (Table 1, Eq. (1)). Turtle bones were likely biased by diagenetic alteration and thus do not represent original lake water values. Using the lake $\delta^{18}O_{H_2O}$ value of −2‰ and the phosphate–water oxygen isotope equilibrium fractionation equation (Lécuyer et al., 2013) water temperatures around 25 ± 3 °C were calculated from $\delta^{18}O_p$ values (corrected for diagenesis by -1.4‰) of fish bones and scales as well as coprolites, which phosphatised rapidly in the lake water. See the text for detailed discussion of the reconstructed temperatures and applied corrections. Fossil pictures are taken from Gruber and Micklich (2007).

Messel with a similar $\delta^{18}O_{H_2O}$ value, amount of mean annual precipitation (MAP) and relative humidity. During the Eocene polar caps were ice free thus the ice volume effect has shifted seawater (and hence precipitation) $\delta^{18}O_{H_2O}$ values by about $+1 \pm 0.2$‰ (Tindall et al., 2010 and references therein) between Eocene and modern oceans. Thus 1‰ needs to be subtracted from modern precipitation $\delta^{18}O_{H_2O}$ values to make them comparable to the values reconstructed for Messel. Hong Kong has climatic conditions ($\delta^{18}O_{H_2O\ weighted\ mean}$: −6.2‰, MAP: 2218 mm, relative humidity: 77%; IAEA/WMO, 2006) very similar as those reconstructed for Messel. Furthermore, Hong Kong is situated in a humid subtropical Cfa climate as it has also been postulated to prevail at Messel (Wilde, 1989; Grein et al., 2011a). The MAT of 22.5 °C for Hong Kong matches perfectly the MAT around 22 °C reconstructed for Messel from plant fossils (Grein et al., 2011a). Guangzhou in SW China ($\delta^{18}O_{H_2O\ weighted\ mean}$: −5‰, MAP: 1724 mm, relative humidity: 68%; IAEA/WMO, 2006) with a MAT of 22.2 °C would be another good modern climatic analogue for Messel. Guangzhou is situated in the same Cfa climatic zone, only 120 km inland NE of Hong Kong. This demonstrates that mammalian drinking water $\delta^{18}O_{H_2O}$ values of -5 ± 1‰ for Messel fit empirically well with a MAT of around 22 °C for extant settings with a Cfa climate. Furthermore, similar MATs around 20 °C were also reconstructed for early Eocene coastal/continental sites at the latitude of Messel (~46°N) using global circulation models (GCMs) (Tindall et al., 2010; Huber and Caballero, 2011). However, enamel $\delta^{18}O_p$ values from more terrestrial mammals with different water use strategies need to be analysed to better constrain the meteoric water $\delta^{18}O_{H_2O}$ values and hence MAT of Messel. Analysis of hydrogen isotopes in plant wax biomarkers from well-preserved leaf cuticles as well as clumped isotope analysis from fish scale bioapatite or authigenic siderite can further help to refine temperature reconstructions for Messel.

6.2.3.2. Water temperature of Lake Messel. Taking the reconstructed preliminary lake water $\delta^{18}O_{H_2O}$ value of about −2‰ water temperatures can be calculated from $\delta^{18}O_p$ values of fish scales and phosphatised coprolites using a phosphate–water oxygen isotope fractionation equation (Lécuyer et al., 2013, Table 1: Eq. (6)). Water temperatures of 19.1 ± 2.6 °C (fish scales/bones) and 18.2 ± 3.3 °C (coprolites) were obtained. These represent minimum estimates because diagenesis has likely also shifted $\delta^{18}O_p$ values of fish bones and scales as well as coprolites to higher values, which will bias reconstructed temperatures towards cooler temperatures. If we assume that the enamel–dentine offset of 1.4‰ for the crocodile tooth reflects the effect of diagenesis on bioapatite $\delta^{18}O_p$ values of aquatic vertebrates and correct for it, warmer water temperatures of 25.4 ± 2.6 °C (fish scales/bones) and 24.5 ± 3.3 °C (coprolites) are calculated (Fig. 6). These temperatures are presumably more realistic although, depending on the degree of diagenetic alteration, and the initial $\delta^{18}O_p$ value of the specimen, they might have been also somewhat lower or higher. Water temperatures of Lake Messel were thus presumably between 19 and 25 °C. These water temperatures are in good agreement with palaeobotanical MAT reconstructions for the middle and early Eocene of about 22 °C for Messel (Grein et al., 2011a) and about 24 °C for the Geiseltal (Mosbrugger et al., 2005), respectively. However, these temperature estimates from aquatic vertebrate remains are preliminary and need confirmation by further $\delta^{18}O_p$ analyses, for instance, of less altered enamel-like ganoid from fish scales. Nevertheless, the temperature data seem to suggest that the oxygenated surface water of Lake Messel, where the fish lived and

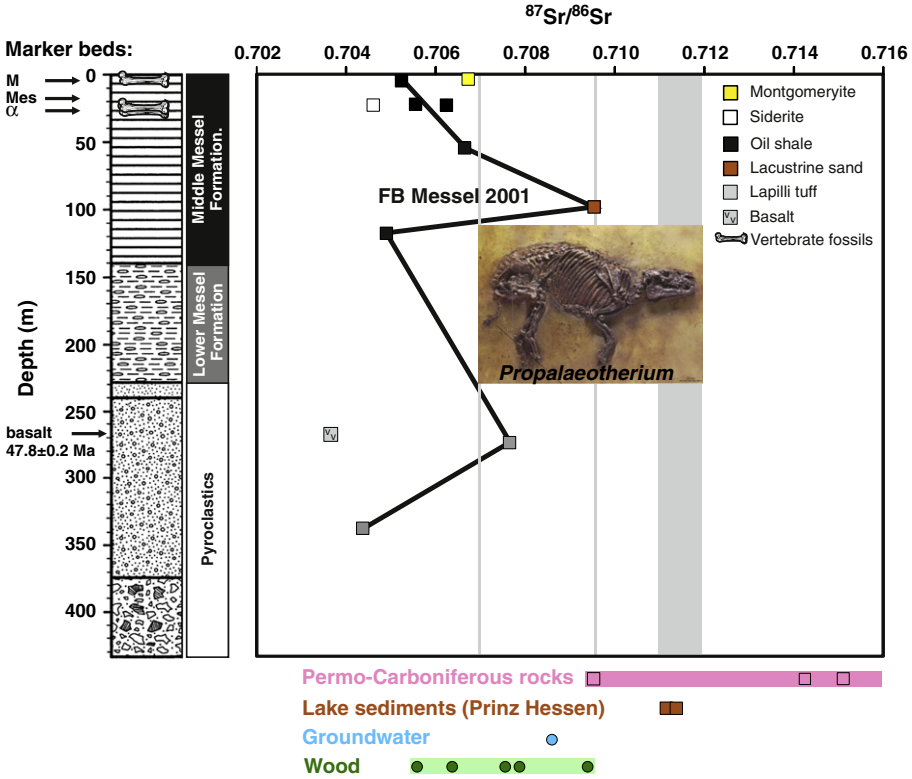

Fig. 7. Strontium isotope composition of rock samples from the Messel FB 2001 research drill core which are connected by a solid line, other samples are from excavations, except the basalt that also comes from the drill core (Table 4). The simplified lithology of the FB 2001 is taken from Mertz and Renne (2005) and the thickness of the middle and lower Messel Formation is given after Felder and Harms (2004). The stratigraphic position of fossils analysed in this study is marked with bone symbols in the oil shale of the upper Middle Messel Formation. Marker beds in the oil shale (M = montgomeryite, Mes = double messelite layer, α = siderite layer) are given after Neubert (1999) the Ar–Ar age of the basalt is from Mertz and Renne (2005). Data of rock samples from other drill cores in the surrounding of the Messel Pit (see text for details) as well as wood samples collected on different bedrock substrates in the Messel Pit are given for comparison. The $^{87}Sr/^{86}Sr$ ranges of the six *Propalaeotherium* teeth are plotted as vertical grey bars, assuming to represent the bioavailable $^{87}Sr/^{86}Sr$ of the Eocene land surface in the surrounding of Lake Messel.

mineralised their hard tissues, had similar water temperatures as the air temperature, which is to be expected. If indeed coprolites phosphatised predominantly during early diagenesis in the anoxic bottom water at the lake floor, then bottom and surface water temperatures were similar in Lake Messel. This is not unusual because tropical lakes often have no pronounced temperature gradients between epi- and hypolimnion (Wetzel, 1983; Rabenstein et al., 2004).

6.3. Strontium isotopes: fingerprint of habitat versus diagenetic alteration

6.3.1. Aquatic vertebrates

The oil shales from different stratigraphical levels in the Messel FB 2001 drill core yielded similar $^{87}Sr/^{86}Sr$ of about 0.705 to 0.706 (Fig. 7). These low values reflect Sr input from the weathering of the basaltic pyroclastics from the maar eruption. Mantle-derived Eocene low SiO_2 melts in the realm of the Sprendlinger Horst have low $^{87}Sr/^{86}Sr$ of 0.7032 to 0.7038 (n = 6; pers. comm. D.F. Mertz 2014; Fig. 3). A similar value of 0.70365 was measured for the Ar–Ar dated basalt fragment from the lapilli tuff. The lapilli tuff samples from the FB 2001 Messel drill core have more radiogenic $^{87}Sr/^{86}Sr$ of 0.70438 and 0.70766 (Fig. 7), due to the variable admixture of surrounding crustal bedrock during the phreatomagmatic eruption. This basaltic and admixed crustal material plus weathering products thereof contribute a significant part of the clay mineral fraction of the oil shale, mainly smectites (Weber, 1991). Strontium released from the pyroclastic rocks led to a lake water $^{87}Sr/^{86}Sr$ of 0.705 ± 0.01, which is reflected in the authigenic phosphate (montgomeryite, messelite) and carbonate (siderite) minerals (Table 3; Fig. 3). These minerals precipitated from the lake bottom water and occur dispersed in the sediment or form laminae and sometimes even marker beds or concretions around fossils (Felder and Gaupp, 2006; Felder, 2007). Aquatic vertebrates have either incorporated the Sr isotope composition from the lake water in vivo and/or post-mortem from pore water fluids. Both processes should result in similar $^{87}Sr/^{86}Sr$ ratios. Thus bones and scales of fish, turtles and crocodiles have low $^{87}Sr/^{86}Sr$ in the range of 0.704 to 0.706. A post mortem Sr uptake is very likely because bone is prone to diagenetic trace element exchange (Trueman and Tuross, 2002), especially Sr (Nelson et al., 1986; Budd et al., 2000; Hoppe et al., 2003). Furthermore, the positive $\delta^{13}C$ values of these specimens indicate a diagenetic overprint (Fig. 3). Thus bone and dentine in Messel are both affected by significant diagenetic alteration, especially the trace elements such as Sr and others (see Fig. 8).

6.3.2. Terrestrial vertebrates: Propalaeotherium

In contrast, the enamel of the terrestrial hippomorph *Propalaeotherium* has much higher $^{87}Sr/^{86}Sr$ of ~0.711 except for two teeth with lower values of 0.70713 and 0.70972 (Fig. 7). These values would be consistent with these animals living on non-basaltic bedrock substrates with more elevated bioavailable $^{87}Sr/^{86}Sr$. Hence at the time *Propalaeotherium* dwelled the forested landscape around the Lake Messel the initial tuff ring deposits around the crater, formed 640 ka beforehand during the phreatomagmatic eruption, were probably already eroded away or – if still present – the crater wall was not the preferred habitat of *Propalaeotherium*. The Messel maar is surrounded by Upper Permian (Rotliegend) sediments, predominantly siliciclastic red beds, as well as Carboniferous igneous rocks such as granites, granodiorites, and diorites (Marell, 1989; Mezger et al., 2013). These Palaeozoic rocks represent the presumable bedrock substrate on which *Propalaeotherium* lived. However, $^{87}Sr/^{86}Sr$ measured for Permian rocks are significantly higher (0.714 to 0.723, Fig. 3) and those for Carboniferous diorites and granodiorites as well as modern wood are lower ≤0.7093 than most enamel values of *Propalaeotherium* (~0.711). However, silty to sandy Eocene lake sediments from Messel and the nearby Grube Prinz von Hessen oil shale pit have similar $^{87}Sr/^{86}Sr$ of 0.7095 to 0.711, respectively. These sediments represent the siliciclastic detritus of the weathering Eocene land surface and their $^{87}Sr/^{86}Sr$ match well with the *Propalaeotherium* enamel values (Fig. 3). Two teeth had a significantly lower enamel $^{87}Sr/^{86}Sr$ of 0.7071 and 0.7097 still being higher than $^{87}Sr/^{86}Sr$ of basaltic Eocene volcanic rocks (~0.703) and the oil shale (~0.706). This could reflect some diagenetic alteration of the enamel towards the pore water/oil shale $^{87}Sr/^{86}Sr$ values. However, the carbonate content of the enamel is not affected by diagenesis (unlike dentine of the other *Propalaeotherium* teeth, Fig. 5) because the enamel still has a C_3 plant feeder $\delta^{13}C$ signature (Fig. 3). To alter the carbon isotope composition of enamel a high water/apatite ratio is necessary (Wang and Cerling, 1994). Thus Sr is presumably more susceptible to diagenetic alteration than $\delta^{13}C$ of the enamel carbonate. On the other hand the lower $^{87}Sr/^{86}Sr$ of 0.7071 and 0.7097 could still represent an in vivo value as they fall in the $^{87}Sr/^{86}Sr$ range (0.7056 to 0.7094) of wood samples from modern trees growing on Permo-Carboniferous mafic and felsic crystalline bedrocks (diorite and granite) in the Messel pit (Figs. 3 and 7, Table 4). Overall the Sr isotope data corroborate that *Propalaeotherium* lived predominantly on a Palaeozoic bedrock substrate and not on Eocene volcanic rocks.

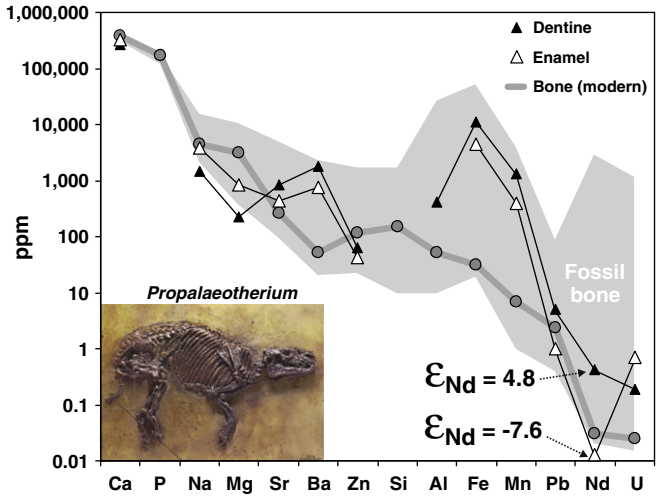

Fig. 8. Element concentrations and Nd isotope composition (ε_{Nd}) of enamel and dentine of a *Propalaeotherium* molar (FZ EQ ME 1, Table 6). For comparison the average element concentrations of bones from different extant mammals as well as various fossil bones from different diagenetic settings are plotted after data from Tütken (2003). It is striking that the enamel still has near-in vivo concentrations of Nd as well as other trace elements such as Sr. The low enamel Nd content supports that no significant diagenetic alteration occurred and explains the unusual preservation of a near-in vivo ε_{Nd} value of −7.6 derived from older crustal rocks in the 47-Myr-old enamel. In contrast in the dentine Nd is 80 times enriched compared to the enamel and has an ε_{Nd} value of +4.8, indicating a diagenetic uptake of mantle-derived Nd from the lake/pore water during diagenesis. Other elements such as Fe, Mn and U are diagenetically enriched, both in the enamel and dentine.

6.4. Diagenesis: preservation of enamel and alteration of dentine isotope signatures

Diagenetic exchange with Messel lake water caused low $^{87}Sr/^{86}Sr$ ~0.706 and high $\delta^{13}C$ >10‰, bioapatite values as indicated by isotope compositions of authigenic phosphate minerals such as messelite and montgomeryite (Fig. 3). Dentine samples of two *Propalaeotherium* teeth have such low $^{87}Sr/^{86}Sr$ values while their enamel still has high $^{87}Sr/^{86}Sr$ of 0.711–0.712 (Fig. 3). Thus dentine of these teeth suffered from post mortem Sr exchange (Fig. 8), while enamel of the same teeth still preserved near-in vivo values. However, even in the enamel some minor diagenetic alteration and element exchange with ambient pore water seems to have occurred because enamel samples are shifted slightly towards lower $^{87}Sr/^{86}Sr$ and higher $\delta^{13}C$ values (Fig. 3). This indicates probably a small degree of diagenetic alteration of both Sr and C isotope compositions. Overall the combined $\delta^{13}C$ and $^{87}Sr/^{86}Sr$ analyses can be used to monitor for diagenetic alteration and do indicate preservation of near-in vivo isotopic compositions in enamel, while dentine

values are clearly diagenetically altered. Enamel $^{87}Sr/^{86}Sr$ seem still to reflect the bioavailable Sr isotope compositions of the Eocene land surface about 47 Ma ago and enable to study habitat use and mobility of the terrestrial Messel vertebrates, while enamel $\delta^{13}C$ values allow to determine their feeding ecology.

6.4.1. Exceptional geochemical preservation of enamel: REE contents and Nd isotopes

The very good geochemical preservation of enamel is further supported by trace element and Nd isotope ($^{143}Nd/^{144}Nd$, expressed as ε_{Nd} value) analyses of a *Propalaeotherium* tooth (FZ EQ ME 1). Rare earth elements (REE) such as Nd (i.e. the $^{143}Nd/^{144}Nd$ ratio) are important tracers for palaeoceanography, water provenance and redox conditions (Elderfield and Greaves, 1982; Elderfield and Sholkovitz, 1987; Grandjean et al., 1987) as well as fossil provenance (Trueman and Benton, 1997; Tütken et al., 2011), which can be incorporated into biogenic apatite during fossilisation (Henderson et al., 1983; Elderfield and Pagett, 1986; Grandjean et al., 1987; Trueman and Tuross, 2002). Because REE concentrations in fresh bones and teeth are in the lower ppb-level range but are enriched in fossil bioapatite during diagenesis in large quantities up to 1–1000 ppm they are sensitive tracers for diagenetic alteration of bioapatite (Henderson et al., 1983; Lécuyer et al., 2003; Herwartz et al., 2011, 2013b). REE uptake starts immediately post mortem (Trueman et al., 2004; Kohn and Moses, 2013) and lasts over geological time scales of millions of years (Kocsis et al., 2010; Herwartz et al., 2011, 2013a). REE concentrations in enamel are still low in the ppb range, similar to fresh bone, while dentine has already 80 times higher contents at the ppm level (Fig. 8). Enamel has a negative ε_{Nd} value of −7.6 while dentine of the same tooth has a positive ε_{Nd} value of 4.9, similar to that of a crocodile bone ($\varepsilon_{Nd} = 4.8$) and its embedding oil shale ($\varepsilon_{Nd} = 3.8$) (Table 6; Tütken et al., 2011). The huge difference of 12.5 ε_{Nd} units between enamel and dentine of the same tooth is surprising because the Nd isotope composition of fossil bones and teeth usually reflects that of the embedding sediment (i.e. diagenetic fluid) from which the Nd is incorporated during diagenesis (Tütken et al., 2011). Reworked specimens may deviate from this relationship (Tütken et al., 2011), however, reworking is obviously no explanation given the taphonomic situation of the Messel conservation Lagerstätte. Hence the low ε_{Nd} value of the enamel still reflects remnants of the in vivo Nd isotope composition incorporated by the *Propalaeotherium*. Negative ε_{Nd} values are expected for older crustal rocks and sediments derived from these by weathering while positive ε_{Nd} values are typical for mantle-derived young volcanic rocks such as basalts (e.g., Goldstein and Jacobsen, 1988). Thus the low enamel ε_{Nd} value of −7.6 still reflects, at least partially, the isotopic composition of the bioavailable Nd ingested in vivo by the *Propalaeotherium* on its presumable Palaeozoic bedrock substrate. In contrast, the dentine has clearly incorporated mantle-derived Nd with a positive ε_{Nd} value of around 4 during fossilisation in the volcanically influenced lake water. The positive ε_{Nd} values indicate that the REE budget of the lake water was mainly controlled by weathering of basaltic tuff material.

Overall enamel of *Propalaeotherium* teeth from Messel has preserved near-in vivo C, O, Sr and probably even Nd isotope signatures. This indicates an exceptional preservation of the enamel apatite of Messel vertebrate fossils and opens good perspectives for quantitative geochemical reconstructions of vertebrate palaeobiology and palaeoenvironment of the middle Eocene Messel ecosystem.

7. Conclusions

A combined multi-isotope (C, O, Sr, Nd) approach demonstrates that enamel apatite of fossil vertebrates from Messel is geochemically exceptionally well-preserved, while dentine and bone are clearly diagenetically altered. In Messel diagenetic end member values of the volcanically influenced and through methanogenesis ^{12}C-depleted anoxic bottom water of the Eocene maar lake setting are isotopically very distinct from in vivo bioapatite values of terrestrial vertebrates. This unique taphonomic setting allows assessing the geochemical preservation of the 47-Myr-old Messel vertebrate fossils.

Enamel of the terrestrial hippomorph perissodactyl *Propalaeotherium* still has:

(1) $\delta^{13}C$ values around $-9 \pm 1‰$ expected for a C_3 plant feeder while dentine of the same teeth is clearly diagenetically altered and has about 15–17‰ higher $\delta^{13}C$ values (5.6‰ and 8.6‰) being amongst the highest bioapatite $\delta^{13}C$ values for terrestrial vertebrates reported so far.
(2) $^{87}Sr/^{86}Sr$ ~0.711 ± 0.001 typical for Palaeozoic crustal rocks surrounding Messel while dentine has an unradiogenic, volcanically influenced $^{87}Sr/^{86}Sr$ of ~0.706 similar to that of the embedding Middle Eocene oil shale.
(3) ε_{Nd} value of around −7.6 while the dentine of the same tooth has a high ε_{Nd} value of 4.8 indicating diagenetic uptake of mantle-derived Nd; the low ε_{Nd} in enamel suggests even a partial preservation of in vivo Nd isotope composition; this is very unusual but further supported by low REE contents in enamel compared to the dentine.

Isotope analysis of enamel from Messel vertebrates can thus reliably be used to reconstruct their diet, drinking water and habitat use. The enamel Sr, C and O isotope compositions of the *Propalaeotherium* indicate that it lived on Palaeozoic bedrock substrate, fed in a C_3 plant ecosystem and drank meteoric water with an average $\delta^{18}O_{H_2O}$ value of around $-5 \pm 1‰$. This value is depleted compared to the preliminary estimate for the lake water of around −2‰. The ^{18}O-enriched water of Lake Messel was probably not a major source of drinking water for *Propalaeotherium*. Preliminary temperature estimates from $\delta^{18}O_p$ values of *Propalaeotherium* enamel and fish bones/scales using according transfer functions yielded a MAT of around 18 ± 2.5 °C and a lake surface water temperature of around 25 ± 3 °C, respectively. These values are in good agreement with MAT estimates from fossil plant remains with the former value being at the lower and the latter at the upper end of palaeobotanical temperature estimates for Messel.

Propalaeotherium enamel $^{87}Sr/^{86}Sr$ of around 0.711 indicates that the basaltic tuff ring of the maar was not present anymore about 640 ka after the phreatomagmatic eruption and diatreme formation or at least was not its preferred habitat.

Overall this geochemical taphonomic study demonstrates that isotope analysis of vertebrate fossils from Messel are very promising and will provide new insights into the palaeoenvironment and palaeoecology of the fauna and contribute to a better understanding of the taphonomy and fossilisation processes in Lake Messel. Isotope research to

Table 6
Nd isotope composition of vertebrate fossils and embedding oil shale of Messel.

Sample-nr.	Taxon	Material	Skeletal element	Specimen-nr.	$^{143}Nd/^{144}Nd$	SD (ppm)	$\varepsilon_{Nd(0)}$
FZ EQ ME 1	*Propalaeotherium hassiacum*	Enamel	M indet.	HLMD ME 144	0.512249	23	−7.6
FD EQ ME 1	*Propalaeotherium hassiacum*	Dentine	M indet.	HLMD ME 144	0.512888	8	4.9
FK KR ME 1	*Diplocynodon darwini*	Bone		SMF-ME 11284	0.512885	8	4.8
SED ME 1		Oil shale		SMF-ME 11284	0.512834	9	3.8

reconstruct the food web, habitat use and niche partitioning of vertebrates in and around Lake Messel are ongoing.

Acknowledgements

I thank Sonja Wedmann and Stephan Schaal from the Senckenberg Messel Forschung for kind access to fossil material from ongoing excavations in the Messel pit. Elvira Brahm from the Senckenberg Messel Forschung is acknowledged for providing stratigraphic information of the fossils. I am especially grateful to Franz-Jürgen Harms for the possibility to take rock samples from the 2001 Messel research drill core and other drill cores in the Messel core storage site as well as for insightful explanations of the geology of the Messel pit and its surrounding as well as a guided tour to the pit for wood sampling in 2008. Norbert Micklich and Oliver Sandrock are acknowledged for access to teeth of *Propalaeotherium* in the Hessische Landesmuseum Darmstadt. Michael Wuttke (Erdgeschichtliche Denkmalpflege Rheinland-Pfalz) for the montgomeryite and messelite samples as well as information about Messel and comments on the manuscript. Dieter Mertz (University of Mainz) is acknowledged for the unpublished Sr isotope data of Eocene low SiO_2 volcanic rocks from the Sprendlinger Horst. I thank Philipp Hermann for help with sample preparation for isotope analyses. Carsten Münker and Frank Wombacher are acknowledged for access to the clean lab and MC–ICP-MS facilities at the Steinmann Institute of the University of Bonn. I thank Bernd Steinhilber and Elmar Reitter for running the stable isotope and TIMS Nd isotope analyses, respectively, both at the University of Tübingen. Christophe Lécuyer and François Fourel (University of Lyon) were so kind to run phosphate oxygen isotope analyses of some samples. Klaus Simon (University of Göttingen) is acknowledged for the trace element analyses of the *Propalaeotherium* tooth. Special thanks to Matthew Kohn for fruitful discussion of the oxygen isotope data, horse physiology and air temperature calculations. I thank Christophe Lécuyer, Laszlo Kocsis and an anonymous reviewer, whose constructive comments helped to significantly improve the manuscript. Olaf Lenz was so kind to provide corel draw files for Fig. 1. Antoine Zazzo is acknowledged for its patience and the efficient editorial handling of the manuscript as well as for organising the 7th Bone diagenesis meeting in Lyon and this special issue together with Vincent Balter. Kate Britton (University of Aberdeen) is acknowledged for comments on the manuscript and for proof-reading the English. This research was funded by the DFG grant TU 148/2-1 for the Emmy Noether Group “Bone Geochemistry” to TT.

References

Ambrose, S.H., Norr, L., 1993. Experimental evidence for the relationship of the carbon isotope ratios of whole diet and dietary protein to those of bone collagen and carbonate. In: Lambert, J., Grupe, G. (Eds.), Prehistoric Human Bone, Archaeology at the Molecular Level. Springer, Berlin, pp. 1–37.

Amiot, R., Lécuyer, C., Buffetaut, E., Fluteau, F., Legendre, S., Martineau, F., 2004. Latitudinal temperature gradient during the Cretaceous n–Middle Maastrichtian: $\delta^{18}O$ record of continental vertebrates. Earth Planet. Sci. Lett. 226, 255–272.

Amiot, R., Lécuyer, C., Escarguel, G., Billon-Bruyat, J.-P., Buffetaut, E., Langlois, C., Martin, S., Martineau, F., Mazin, J.-M., 2007. Oxygen isotope fractionation between crocodilian phosphate and water. Palaeogeogr. Palaeoclimatol. Palaeoecol. 243, 412–420.

Arppe, L., Karhu, J.A., Vartanyan, S.L., 2009. Bioapatite $^{87}Sr/^{86}Sr$ of the last woolly mammoths — implications for the isolation of Wrangel Island. Geology 37, 347–350.

Bahrig, B., 1989. Stable isotope composition of siderite as an indicator of paleoenvironmental history of oil shale lakes. Palaeogeogr. Palaeoclimatol. Palaeoecol. 70, 139–151.

Balter, V., 2004. Allometric constraints on Sr/Ca and Ba/Ca partitioning in terrestrial mammalian trophic chains. Oecologia 139, 83–88.

Balter, V., Telouk, P., Reynard, B., Braga, J., Thackeray, F., Albarède, F., 2008. Analysis of coupled Sr/Ca and $^{87}Sr/^{86}Sr$ variations in enamel using laser-ablation tandem quadrupole-multicollector ICPMS. Geochim. Cosmochim. Acta 72, 3980–3990.

Barrick, R.E., Fischer, A.G., Showers, W.J., 1999. Oxygen isotopes from turtle bone: applications for terrestrial paleoclimates? Palaios 14, 186–191.

Bauersachs, T., Schouten, S., Schwark, L., 2014. Characterization of the sedimentary organic matter preserved in Messel oil shale by bulk geochemistry and stable isotopes. Palaeogeogr. Palaeoclimatol. Palaeoecol. 410, 390–400.

Beard, B.L., Johnson, C.M., 2000. Strontium isotope composition of skeletal material can determine the birth place and geographic mobility of humans and animals. J. Forensic Sci. 45, 1049–1061.

Bentley, R.A., 2006. Strontium isotopes from the earth to the archaeological skeleton: a review. J. Archaeol. Method Theory 13, 135–187.

Berg, D.E., 1964. Krokodile als Klimazeugen. Geol. Rundsch. 54, 328–333.

Blum, J.D., Taliaferro, E.H., Weisse, M.T., Holmes, R.T., 2000. Changes in Sr/Ca, Ba/Ca and $^{87}Sr/^{86}Sr$ ratios between two forest ecosystems in the northeastern U.S.A. Biogeochemistry 49, 87–101.

Britton, K., Grimes, V., Dau, J., Richards, M.P., 2009. Reconstructing faunal migrations using intra-tooth sampling and strontium and oxygen isotope analyses: a case study of modern caribou (*Rangifer tarandus granti*). J. Archaeol. Sci. 36, 1163–1172.

Britton, K.H., Grimes, V., Niven, L., Steele, T., McPherron, S., Soressi, M., Kelly, T., Jaubert, J., Hublin, J.-J., Richards, M., 2011. Strontium isotope evidence for migration in late Pleistocene Rangifer: implications for Neanderthal hunting strategies at the Middle Palaeolithic site of Jonzac, France. J. Hum. Evol. 61, 176–185.

Bryant, J.D., Froelich, P.N., 1995. A model of oxygen isotope fractionation in body water of large mammals. Geochim. Cosmochim. Acta 59, 4523–4537.

Budd, P., Montgomery, J., Barreiro, B., Thomas, R.G., 2000. Differential diagenesis of strontium in archaeological human dental tissues. Appl. Geochem. 15, 687–694.

Cerling, T.E., Harris, J.M., 1999. Carbon isotope fractionation between diet and bioapatite in ungulate mammals and implications for ecological and paleoecological studies. Oecologia 120, 347–363.

Cerling, T.E., Wang, Y., Quade, J., 1993. Expansion of C4 ecosystems as an indicator of global ecological change in the Late Miocene. Nature 361, 344–345.

Cerling, T.E., Harris, J.M., MacFadden, B.J., Leakey, M.G., Quade, J., Eisenmann, V., Ehleringer, J.R., 1997. Global vegetation change through the Miocene–Pliocene boundary. Nature 389, 153–158.

Cerling, T.E., Hart, J.A., Hart, T.B., 2004. Stable isotope ecology in the Ituri Forest. Oecologia 138, 5–12.

Chappe, W., Albrecht, W., Michaelis, W., 1982. Polar lipids of Archaebacteria in sediments and petroleums. Science 217, 65–66.

Chenery, C., Müldner, G., Evans, J., Eckardt, H., Lewis, M., 2010. Strontium and stable isotope evidence for diet and mobility in Roman Gloucester, UK. J. Archaeol. Sci. 37, 150–163.

Collinson, M.E., Manchester, S.R., Wilde, V., 2012. Fossil fruits and seeds of the Middle Eocene Messel biota, Germany. Abh. Senckenberg. Ges. Naturforsch. 570, 1–251.

Copeland, S.R., Sponheimer, M., de Ruiter, D.J., Lee-Thorp, J.A., Codron, D., le Roux, P.J., Grimes, V., Richards, M.P., 2011. Strontium isotope evidence for landscape use by early hominins. Nature 474, 76–78.

D'Angela, D., Longinelli, A., 1990. Oxygen isotopes in living mammal's bone phosphate: further results. Chem. Geol. 86, 75–82.

Dansgaard, W., 1964. Stable isotopes in precipitation. Tellus 16, 436–468.

Delgado Huertas, A., Iacumin, P., Stenni, B., Sánchez Chillón, B., Longinelli, A., 1995. Oxygen isotope variations of phosphate in mammalian bone and tooth enamel. Geochim. Cosmochim. Acta 59, 4299–4305.

DeNiro, M.J., Epstein, S., 1978. Influence of diet on the distribution of carbon isotopes in animals. Geochim. Cosmochim. Acta 42, 495–506.

Diefendorf, A.F., Mueller, K.E., Wing, S.L., Koch, P.L., Freeman, K.H., 2010. Global patterns in leaf ^{13}C discrimination and implications for studies of past and future climate. Proc. Natl. Acad. Sci. 107, 5738–5743.

Eccarius, B., Frechen, M., Harms, F.-J., 2005. Neue Attraktion in der Grube Messel: Forschungsbohrung 2001 als artesischer Brunnen. Nat. Mus. 135, 167–172.

Elderfield, H., Greaves, M.J., 1982. The rare earth elements in seawater. Nature 296, 214–219.

Elderfield, H., Pagett, R., 1986. Rare Earth elements in Ichthyoliths: variations with redox conditions and depositional environment. In: Riley, J.P. (Ed.), Sciences of the Total Environment, pp. 175–197.

Elderfield, H., Sholkovitz, E.R., 1987. Rare earth elements in pore water of reducing nearshore sediments. Earth Planet. Sci. Lett. 82, 280–288.

Farquhar, G.D., Ehleringer, J.R., Hubick, K.T., 1989. Carbon isotope discrimination and photosynthesis. Annu. Rev. Plant Physiol. Plant Mol. Biol. 40, 503–537.

Felder, M., 2007. Phosphatminerale im Messeler Ölschiefer. In: Mosbrugger, V. (Ed.), Senckenberg 2005-2006, pp. 38–39.

Felder, M., Gaupp, R., 2006. The $\delta^{13}C$ and $\delta^{18}O$ signatures of siderite — a tool to discriminate mixis patterns in ancient lakes. Z. Dtsch. Ges. Geowiss. 157, 387–410.

Felder, M., Harms, F.-J., 2004. Lithologie und genetische Interpretation der vulkanosedimentären Ablagerungen aus der Grube Messel anhand der Forschungsbohrung Messel 2001 und weiterer Bohrungen. Cour. Forschungs-Inst. Senckenberg. 252, 151–203.

Feranec, R.S., MacFadden, B.J., 2006. Isotopic discrimination of resource partitioning among ungulates in C_3-dominated communities from the Miocene of Florida and California. Paleobiology 32, 191–205.

Feranec, R.S., Hadly, E.A., Paytan, A., 2007. Determining landscape use of Holocene mammals using strontium isotopes. Oecologia 153, 943–950.

Fox-Dobbs, K., Wheatley, P.V., Koch, P.L., 2006. Carnivore specific bone apatite and collagen carbon isotope fractionations, case studies of modern and fossil grey wolf populations. Eos Transactions, AGU 87, Fall Meeting Suppl., B53C–B0366C.

Franzen, J.L., 1995. Die Equoidea des europäischen Mitteleozäns (Geiseltalium). Hallesches Jahrbuch für Geowissenschaften, Reihe Geol. Paläontol. Miner. 17, 31–45.

Franzen, J.L., 2005. The implications of the numerical dating of the Messel fossil deposit (Eocene, Germany) for mammalian biochronology — Conséquences de la datation de l'âge numérique du gisement de Messel (Eocéne, Allemagne) pour la biochronologie des mammifères. Ann. Paléontologie 91, 329–335.

Franzen, J.L., 2006. *Eurohippus parvulus parvulus* (Mammalia, Equidae) aus der Grube Prinz von Hessen bei Darmstadt (Süd-Hessen, Deutschland). Senckenb. Lethaea 86, 265–269.

Franzen, J.L., 2007. Eozäne Equoidea (Mammalia, Perissodactyla) aus der Grube Messel bei Darmstadt (Deutschland), Funde der Jahre 1969–2000. Schweiz. Paläontol. Abh. 127, 1–245.

Franzen, J.L., Weber, J., Wuttke, M., 1982. Senckenberg-Grabungen in der Grube Messel bei Darmstadt. 3. Ergebnisse 1979–1981. Cour. Forschungs-Inst. Senckenberg. 54, 1–118.

Fricke, H.C., O'Neil, J.R., 1999. The correlation between $^{18}O/^{16}O$ ratios of meteoric water and surface temperature: its use in investigating terrestrial climate change over geologic time. Earth Planet. Sci. Lett. 170, 181–196.

Fricke, H.C., Rogers, R.R., Backlund, R., Dwyer, C.N., Echt, S., 2008. Preservation of primary stable isotope signals in dinosaur remains, and environmental gradients of the Late Cretaceous of Montana and Alberta. Palaeogeogr. Palaeoclimatol. Palaeoecol. 266, 13–27.

Gehler, A., Tütken, T., Pack, A., 2011. Triple oxygen isotope analysis of bioapatite as tracer for diagenetic alteration of bones and teeth. Palaeogeogr. Palaeoclimatol. Palaeoecol. 310, 84–91.

Goldstein, S.J., Jacobsen, S.B., 1988. Nd and Sr isotopic systematics of river water suspended material: implications for crustal evolution. Earth Planet. Sci. Lett. 87, 249–265.

Goth, K., 1990. Der Messeler Ölschiefer – ein Algenlaminit. Cour. Forschungs-Inst. Senckenberg. 131, 1–143.

Grandjean, P., Cappetta, H., Michard, A., Albarède, F., 1987. The assessment of REE patterns and $^{143}Nd/^{144}Nd$ ratios in fish remains. Earth Planet. Sci. Lett. 84, 181–196.

Grein, M., Roth-Nebelsick, A., Wilde, V., 2010. Carbon isotope composition of middle Eocene leaves from the Messel Pit, Germany. Palaeodiversity 3, 1–7.

Grein, M., Utescher, T., Wilde, V., Roth-Nebelsick, A., 2011a. Reconstruction of the middle Eocene climate of Messel using palaeobotanical data. Neues Jb. Geol. Paläontol. Abh. 260, 305–318.

Grein, M., Konrad, W., Wilde, V., Utescher, T., Roth-Nebelsick, A., 2011b. Reconstruction of atmospheric CO_2 during the early middle Eocene by application of a gas exchange model to fossil plants from the Messel Formation, Germany. Palaeogeogr. Palaeoclimatol. Palaeoecol. 309, 383–391.

Messel — treasures of the Eocene. In: Gruber, G., Micklich, N. (Eds.), Book to the exhibition "Messel on Tour" Darmstadt, Hessisches Landesmuseum.

Harms, F.-J., mit Beiträgen von Aderhold, G., Hoffmann, I., Nix, T., Rosenberg, F., 1999. Erläuterungen zur Grube Messel bei Darmstadt, Südhessen. Schriftenr. Dtsch. Geol. Ges. 8 Kleine Senckenberg.-Reihe 31, 181–222.

Hayes, J.M., Takigiku, R., Ocampo, R., Callot, H.J., Albrecht, P., 1987. Isotopic compositions and probably origins of organic molecules in the Eocene Messel Shale. Nature 329, 48–51.

Heaton, T.H.E., 1999. Spatial, species, and temporal variations in the $^{13}C/^{12}C$ ratios of C_3 plants: implications for paleodiet studies. J. Archaeol. Sci. 26, 637–649.

Henderson, P., Marlow, C.A., Molleson, T.I., Williams, C.T., 1983. Patterns of chemical change during bone fossilization. Nature 306, 358–360.

Herwartz, D., Tütken, T., Münker, C., Jochum, K.-P., Stoll, B., Sander, P.M., 2011. Timescales and mechanisms of REE and Hf uptake in fossil bones. Geochim. Cosmochim. Acta 75, 82–105.

Herwartz, D., Münker, C., Tütken, T., Hoffmann, J.E., Wittke, A., Barbier, B., 2013a. Lu–Hf systematics of fossil biogenic apatite and their effects on geochronology. Geochim. Cosmochim. Acta 101, 328–343.

Herwartz, D., Tütken, T., Jochum, K.-P., Sander, P.M., 2013b. REE systematics of fossil bone revealed by LA–ICPMS. Geochim. Cosmochim. Acta 103, 161–183.

Hoppe, K.A., Koch, P.L., Carlson, R.W., Webb, S.D., 1999. Tracking mammoths and mastodons: reconstruction of migratory behavior using strontium isotope ratios. Geology 27, 439–442.

Hoppe, K.A., Koch, P.L., Furutani, T.T., 2003. Assessing the preservation of biogenic strontium in fossil bones and tooth enamel. Int. J. Osteoarchaeol. 13, 20–28.

Huber, M., Caballero, R., 2011. The early Eocene equable climate problem revisited. Clim. Past 7, 603–633.

Hummel, K., 1924. Vulkanisch bedingte Braunkohlenbildung. Braunkohle 1924, 293–298.

Iacumin, P., Bocherens, H., Mariotti, A., Longinelli, A., 1996. Oxygen isotope analyses of coexisting carbonate and phosphate in biogenic apatite: a way to monitor diagenetic alteration of bone phosphate? Earth Planet. Sci. Lett. 142, 1–6.

IAEA/WMO, 2006. Global Network of Isotopes in Precipitation. The GNIP Database, ([WWW Document]) www.iaea.org/water.

Joyce, W.G., Micklich, N., Schaal, S.F.K., Scheyer, T.M., 2012. Caught in the act: the first record of copulating fossil vertebrates. Biol. Lett. 8, 846–848.

Kelts, K., Talbot, M., 1990. Lacustrine carbonates as geochemical archives of environmental change and biotic/abiotic interactions. In: Tilzer, M.M., Serruya, C. (Eds.), Large Lakes: Ecological Structure and Function. Springer, Berlin, pp. 288–315.

Kimble, B.J., Maxwell, J.R., Eglinton, G., Albrecht, P., Ensminger, A., Arpino, P., Ourisson, G., 1974. Tri- and tetraterpenoid hydrocarbons in the Messel oil shale. Geochim. Cosmochim. Acta 28, 1165–1181.

Koch, P.L., 2007. Isotopic study of the biology of modern and fossil vertebrates, In: Minchener, R., Lajtha, K. (Eds.), Stable Isotopes in Ecology and Environmental Science, 2nd edition, pp. 99–154 (Oxford 2007).

Kockel, F., 1988. The palaeogeographical maps. In: Vinken, R. (Ed.), The Northwest European Tertiary Basin. Geologisches Jahrbuch. A100, pp. 423–427.

Kocsis, L., Trueman, C.N., Palmer, M.R., 2010. Protracted diagenetic alteration of REE contents in fossil bioapatites: direct evidence from Lu–Hf isotope systematics. Geochim. Cosmochim. Acta 74, 6077–6092.

Kohn, M.J., 1996. Predicting animal $\delta^{18}O$: accounting for diet and physiological adaption. Geochim. Cosmochim. Acta 60, 4811–4830.

Kohn, M.J., 2010. Carbon isotope compositions of terrestrial C_3 plants as indicators of (paleo)ecology and (paleo)climate. Proc. Natl. Acad. Sci. 107, 19691–19695.

Kohn, M.J., Cerling, T.E., 2002. Stable isotope compositions of biological apatite. Rev. Mineral. Geochem. 48, 455–488.

Kohn, M.J., Fremd, T.J., 2007. Tectonic controls on isotope compositions and species diversification, John Day Basin, central Oregon. PaleoBios 27, 48–61.

Kohn, M.J., Moses, R.J., 2013. Trace element diffusivities in bone rule out simple diffusive uptake during fossilization but explain in vivo uptake and release. Proc. Natl. Acad. Sci. 110, 419–424.

Kohn, M.J., Schoeninger, M.J., Valley, J.W., 1996. Herbivore tooth oxygen isotope compositions: effects of diet and physiology. Geochim. Cosmochim. Acta 60, 3889–3896.

Kohn, M.J., Schoeninger, M.J., Barker, W.B., 1999. Altered states: effects of diagenesis on fossil tooth chemistry. Geochim. Cosmochim. Acta 63, 2737–2747.

Kohn, M.J., McKay, M.P., Knight, J.L., 2005. Dining in the Pleistocene—who's on the menu? Geology 33, 649–652.

Kolodny, Y., Luz, B., Navon, O., 1983. Oxygen isotope variations in phosphate of biogenic apatites: I. Fish bone apatite-rechecking the rules of the game. Earth Planet. Sci. Lett. 64, 398–404.

Larson, T.E., Heikoop, J.M., Perkin, G., Chipera, S.J., Hess, M.A., 2008. Pretreatment technique for siderite removal for organic carbon isotope and C:N ratio analysis in geological samples. Rapid Commun. Mass Spectrom. 22, 865–872.

Lécuyer, C., Grandjean, P., O'Neil, J.R., Cappetta, H., Martineau, F., 1993. Thermal excursions in the ocean at the Cretaceous-Tertiary boundary (northern Morocco): $\delta^{18}O$ record of phosphatic fish debris. Palaeogeogr. Palaeoclimatol. Palaeoecol. 105, 235–243.

Lécuyer, C., Bogey, C., Garcia, J.-P., Grandjean, P., Barrat, J.-A., Floquet, M., Bardet, N., Pereda-Superbiola, X., 2003. Stable isotope composition and rare earth element content of vertebrate remains from the Late Cretaceous of northern Spain (Lano): did the environmental record survive? Palaeogeogr. Palaeoclimatol. Palaeoecol. 193, 457–471.

Lécuyer, C., Amiot, R., Touzeau, A., Trotter, J., 2013. Calibration of the phosphate $\delta^{18}O$ thermometer with carbonate–water oxygen isotope fractionation equations. Chem. Geol. 347, 217–226.

Lee-Thorp, J.A., van der Merwe, N.J., 1987. Carbon isotope analysis of fossil bone apatite. S. Afr. J. Sci. 83, 712–715.

Lenz, O.K., Wilde, V., Riegel, W., 2007. Recolonization of a Middle Eocene volcanic site: quantitative palynology of the initial phase of the maar lake of Messel (Germany). Rev. Palaeobot. Palynol. 145, 217–242.

Lenz, O.K., Wilde, V., Riegel, W., Harms, F.-J., 2010. A 600 k.y. record of El Niño–Southern Oscillation (ENSO): evidence for persisting teleconnections during the Middle Eocene greenhouse climate of Central Europe. Geology 38, 627–630.

Lenz, O.K., Wilde, V., Riegel, W., 2011. Short-term fluctuations in vegetation and phytoplankton during the Middle Eocene greenhouse climate: a 640-kyr record from the Messel oil shale (Germany). Int. J. Earth Sci. 100, 1851–1874.

Levin, N.E., Cerling, T.E., Passey, B.H., Harris, J.M., Ehleringer, J.R., 2006. A stable isotope aridity index for terrestrial environments. Proc. Natl. Acad. Sci. 103, 11201–11205.

Longinelli, A., 1984. Oxygen isotopes in mammal bone phosphate: a new tool for paleohydrological and paleoclimatological research? Geochim. Cosmochim. Acta 48, 385–390.

Longinelli, A., Nuti, S., 1973. Revised phosphate–water isotopic temperature scale. Earth Planet. Sci. Lett. 19, 373–376.

Luz, B., Kolodny, Y., 1985. Oxygen isotope variations in phosphate of biogenic apatites, IV. Mammal teeth and bones. Earth Planet. Sci. Lett. 75, 29–36.

Luz, B., Kolodny, Y., Horowitz, M., 1984. Fractionation of oxygen isotopes between mammalian bone phosphate and environmental drinking water. Geochim. Cosmochim. Acta 48, 1689–1693.

MacFadden, B.J., Higgins, P., 2004. Ancient ecology of 15-million-year-old browsing mammals within C_3 plant communities from Panama. Oecologia 140, 169–182.

MacFadden, B.J., Solounias, N., Cerling, T.E., 1999. Ancient diets, ecology, and extinction of 5-million-year-old horses from Florida. Science 283, 824–827.

Marell, D., 1989. Das Rotliegende zwischen Odenwald und Taunus. Geol. Abh. Hess. 89, 1–129.

Markwick, P.J., 1998. Fossil crocodilians as indicators of Late Cretaceous and Cenozoic climates: implications for using palaeontological data in reconstructing palaeoclimate. Palaeogeogr. Palaeoclimatol. Palaeoecol. 137, 205–271.

Matthess, G., 1966. Zur Geologie des Ölschiefervorkommens von Messel bei Darmstadt. Abhandlungen des hessischen Landesumweltamt für Bodenforschung 51, 1–87.

Maurer, A.-F., Galer, S.J.G., Knipper, C., Beierlein, L., Nunn, E.V., Peters, D., Tütken, T., Alt, K. W., Schöne, B.R., 2012. Bioavailable $^{87}Sr/^{86}Sr$ in different environmental samples — effects of anthropogenic contamination and implications for isoscapes in past migration studies. Sci. Total Environ. 433, 216–229.

Mayr, G., 2009. Paleogene Fossil Birds. Springer, Berlin Germany.

McArthur, J.M., Howarth, R.J., Bailey, T.R., 2001. Strontium isotope stratigraphy: LOWESS Version 3: best fit to the marine Sr-isotope curve for 0–509 Ma and accompanying lookup table for deriving numerical age. J. Geol. 109, 155–170.

McNamara, M.E., Briggs, D.E.G., Orr, P.J., Noh, H., Cao, H., 2012. The original colours of fossil beetles. Proc. R. Soc. B 279, 1114–1121.

Mertz, D.F., Renne, P.R., 2005. A numerical age for the Messel fossil deposit (UNESCO world natural heritage site) from $^{40}Ar/^{39}Ar$ dating. Cour. Forschungs-Inst. Senckenberg. 255, 67–75.

Mezger, J.E., Felder, M., Harms, F.-J., 2013. Crystalline rocks in the maar deposits of Messel: key to understand the geometries of the Messel Fault Zone and diatreme and the post-eruptional development of the basin fill. Z. Dtsch. Ges. Geowiss. 164, 639–662.

Michaelis, W., Albrecht, P., 1979. Molecular fossils of *Archaebacteria* in kerogen. Naturwissenschaften 66, 420–422.

Michaelis, W., Jensch, A., Richnow, H.H., Kruse, U., Mycke, B., 1988. Organofazies des Ölschiefers von Messel. Cour. Forschungs-Inst. Senckenberg. 107, 89–103.

Micklich, N., 2012. Peculiarities of the Messel fish fauna and their palaeoecological implications: a case study. Palaeobiodivers. Palaeoenviron. 92, 585–629.

Mosbrugger, V., Utescher, T., Dilcher, D.L., 2005. Cenozoic continental climatic evolution of Central Europe. Proc. Natl. Acad. Sci. 102, 14964–14969.

Müller, W., Fricke, H., Halliday, A.N., McCulloch, M.T., Wartho, J.-A., 2003. Origin and migration of the Alpine Iceman. Science 302, 862–866.
Navarro, N., Lécuyer, C., Montuire, S., Langlois, C., Martineau, F., 2004. Oxygen isotope compositions of phosphate from arvicoline teeth and Quaternary climatic changes, Gigny, French Jura. Quat. Res. 62, 172–182.
Nelson, B.K., DeNiro, M.J., Schoeninger, M.J., DePaolo, D.J., Hare, P.E., 1986. Effects of diagenesis on strontium, carbon, nitrogen and oxygen concentration and isotopic composition of bone. Geochim. Cosmochim. Acta 50, 1941–1949.
Neubert, E., 1999. The Mollusca of the Eocene Lake Messel. Cour. Forschungs-Inst. Senckenberg. 162, 167–181.
Pack, A., Gehler, A., Süssenberger, A., 2013. Exploring the usability of isotopically anomalous oxygen in bones and teeth as paleo-CO_2-barometer. Geochim. Cosmochim. Acta 102, 306–317.
Passey, B.H., Robinson, T.F., Ayliffe, L.K., Cerling, T.E., Sponheimer, M., Dearing, M.D., Roeder, B.L., Ehleringer, J.R., 2005. Carbon isotope fractionation between diet, breath CO_2, and bioapatite in different mammals. J. Archaeol. Sci. 32, 1459–1470.
Pasteris, J.D., Wopenka, B., Valsami-Jones, E., 2008. Bone and tooth mineralization: why apatite? Elements 4, 97–104.
Pellegrini, M., Lee-Thorp, J.A., Donahue, R.E., 2011. Exploring the variation of the δ^{18}Op and δ^{18}Oc relationship in enamel increments. Palaeogeogr. Palaeoclimatol. Palaeoecol. 310, 71–83.
Pouech, J., Amiot, R., Lécuyer, C., Mazin, J.-M., Martineau, F., Fourel, F., 2014. Oxygen isotope composition of vertebrate phosphates from Cherves-de-Cognac (Berriasian, France): environmental and ecological significance. Palaeogeogr. Palaeoclimatol. Palaeoecol. 410, 290–299.
Price, T.D., Burton, J.H., Bentley, R.A., 2002. The characterization of biologically available strontium isotope ratios for the study of prehistoric migration. Archaeometry 44, 117–135.
Rabenstein, R., Usman, R., Schaal, S., 2004. Suche nach rezenten Seen als Modelle für den eozänen Lebensraum von Messel. Cour. Forschungs-Inst. Senckenberg. 252, 115–138.
Richter, G., 1987. Untersuchungen zur Ernährung eozäner Säuger aus der Fossilfundstätte Messel bei Darmstadt. Cour. Forschungs-Inst. Senckenberg. 91, 1–33.
Richter, G., Baszio, S., 2009. Geographic and stratigraphic distribution of spongillids (porifera) and the leit value of spiculites in the Messel Pit fossil site. Palaeobiodivers. Palaeoenviron. 89, 53–66.
Richter, G., Storch, G., 1994. Zur Paläobiologie Messeler Igel. Nat. Mus. 124, 81–90.
Richter, G., Wuttke, M., 1999. *Luthetiospongilla heili* n. gen. n. sp. und die eozäne Spongillidenfauna von Messel. Cour. Forschungs-Inst. Senckenberg. 216, 183–195.
Rietschel, S., 1994. Messel. Ein Maar-See? Mainz. Naturwiss. Arch. Beih. 16, 213–218.
Rose, K.D., 2012. The importance of Messel for interpreting Eocene Holarctic mammalian faunas. Palaeobio. Palaeoenv. 92, 631–647.
Rozanski, K., Araguás-Araguás, L., Gonfiantini, R., 1993. Isotopic patterns in modern global precipitation. In: Swart, P.K., Lohmann, K.C., McKenzie, J., Savin, S. (Eds.), Climate Change in Continental Isotopic Records (Geophysical Monograph 78). American Geophysical Union, Washington D. C., pp. 1–36.
Rozanski, K., Johnsen, S.J., Schotterer, U., Thompson, L.G., 1997. Reconstruction of past climates from stable isotope records of palaeo-precipitation preserved in continental archives. Hydrol. Sci. 42, 725–745.
Rullkötter, J., Littke, R., Hagedorn-Götz, I., Jankowski, B., 1988. Vorläufige Ergebnisse der organisch-geochemischen und organisch-petrographischen Untersuchungen an Kernproben des Messeler Ölschiefers. Cour. Forschungs-Inst. Senckenberg. 107, 37–53.
Schaal, S., Schmitz-Münker, M., Wolf, H.G., 1987. Neue Korrelationsmöglichkeiten von Grabungsstellen in der eozänen Fossillagerstätte Grube Messel. In: Schaal, S. (Ed.), Forschungsergebnisse zu Grabungen in der Grube Messel bei Darmstadt. Courier Forschungsinstitut Senckenberg. 91, pp. 203–211.
Schaal, S., Ziegler, W., 1992. Messel—An Insight Into the History of Life and of the Earth. Clarendon, Oxford, UK.
Schmitz, M., 1991. Die Koprolithen mitteleozäner Vertebraten aus der Grube Messel bei Darmstadt. Cour. Forschungs-Inst. Senckenberg. 137, 1–199.
Schweissing, M.M., Grupe, G., 2003. Stable strontium isotopes in human teeth and bone: a key to migration events of the late Roman period in Bavaria. J. Archaeol. Sci. 30, 1373–1383.
Schweizer, M.K., Steele, A., Toporski, J.K.W., Fogel, M.L., 2007. Stable isotopic evidence for fossil food webs in Eocene Lake Messel. Paleobiology 33, 590–609.
Schwermann, A., Schultz, J., Wuttke, M., 2012. Virtopsy of the controlled decomposition of a dormouse *Eliomys quercinus* as a tool to analyse the taphonomy of *Heterohyus nanus* from Messel (Eocene, Germany). Palaeobiodivers. Palaeoenviron. 92, 29–43.
Sillen, A., Hall, G., Richardson, S., Armstrong, R., 1998. $^{87}Sr/^{86}Sr$ ratios in modern and fossil food-webs of the Sterkfontein Valley: implications for early hominid habitat preference. Geochim. Cosmochim. Acta 62, 2463–2473.
Smith, K., Wuttke, M., 2012. From tree to shining sea: taphonomy of the arboreal lizard *Geiseltaliellus maarius* from Messel, Germany. Palaeobiodivers. Palaeoenviron. 92, 45–65.
Sturm, M., 1978. Maw contents of an Eocene horse (*Propalaeotherium*) out of the oil shale of Messel near Darmstadt (Preliminary report). Cour. Forschungs-Inst. Senckenberg. 30, 20–122.
Talbot, M.R., 1990. A review of the palaeohydrological interpretation of carbon and oxygen isotopic ratios in primary lacustrine carbonates. Chem. Geol. 80, 261–278.
Thiele-Pfeiffer, H., 1988. Die Mikroflora aus dem mitteleozänen Ölschiefer von Messel bei Darmstadt. Palaeontogr. B 211, 1–86.
Tindall, J., Flecker, R., Valdes, P., Schmidt, D.N., Markwick, P., Harris, J., 2010. Modelling the oxygen isotope distribution of ancient seawater using a coupled ocean–atmosphere GCM: implications for reconstructing early Eocene climate. Earth Planet. Sci. Lett. 292, 265–273.
Trueman, C.N., Benton, M.J., 1997. A geochemical method to trace the taphonomic history of reworked bones in sedimentary settings. Geology 25, 263–266.
Trueman, C.N.G., Tuross, N., 2002. Trace elements in recent and fossil bone apatite. Rev. Mineral. Geochem. 48, 489–521.
Trueman, C.N.G., Behrensmeyer, A.K., Tuross, N., Weiner, S., 2004. Mineralogical and compositional changes in bones exposed on soil surfaces in Amboseli National Park, Kenya: diagenetic mechanisms and the role of sediment pore fluids. J. Archaeol. Sci. 31, 721–739.
Tütken, T., 2003. Die Bedeutung der Knochenfrühdiagenese für die Erhaltungsfähigkeit in vivo erworbener Element- und Isotopenzusammensetzungen in fossilen Knochen. Universität Tübingen, 343 pp. Online Dissertation: http://tobias-lib.uni-tuebingen.de/volltexte/2003/962/.
Tütken, T., 2010. Die Isotopenanalyse fossiler Skelettreste – Bestimmung der Herkunft und Mobilität von Menschen und Tieren. In: H. Meller & K.W. Alt (Hrsg.), Anthropologie, Isotopie und DNA – biografische Annäherung an namenlose vorgeschichtliche Skelette. Tagungsband 2. Mitteldeutscher Archäologentag. Tagungen des Landesmuseums für Vorgeschichte Halle, Band 3, 33–51.
Tütken, T., Vennemann, T.W., 2009. Stable isotope ecology of Miocene mammals of Sandelzhausen, Germany. Paläontol. Z. 83, 207–226.
Tütken, T., Vennemann, T.W., 2011. Fossil bones and teeth: preservation or alteration of biogenic compositions? Palaeogeogr. Palaeoclimatol. Palaeoecol. 310, 1–8.
Tütken, T., Vennemann, T.W., Janz, H., Heizmann, H.E.P., 2006. Palaeoenvironment and palaeoclimate of the Middle Miocene lake in the Steinheim basin, SW Germany, a reconstruction from C, O, and Sr isotopes of fossil remains. Palaeogeogr. Palaeoclimatol. Palaeoecol. 241, 457–491.
Tütken, T., Vennemann, T.W., Pfretzschner, H.-U., 2011. Nd and Sr isotope compositions in modern and fossil bones — proxies for vertebrate provenance and taphonomy. Geochim. Cosmochim. Acta 75, 5951–5970.
van der Merwe, N.J., Medina, E., 1991. The canopy effect, carbon isotope ratios and foodwebs in Amazonia. J. Archaeol. Sci. 18, 249–259.
Vennemann, T.W., Fricke, H.C., Blake, R.E., O'Neil, J.R., Colman, A., 2002. Oxygen isotope analyses of phosphates: a comparison of techniques for analysis of Ag_3PO_4. Chem. Geol. 185, 321–336.
Vinter, J., Briggs, D.E.G., Clarke, J., Mayr, G., Prum, R.O., 2010. Structural coloration in a fossil feather. Biol. Lett. 6, 128–131.
von Koenigswald, W., Schaarschmidt, F., 1983. Ein Urpferd aus Messel, das Weinbeeren fraß. Nat. Mus. 113, 79–84.
von Koenigswald, W., Storch, G (Eds.), 1998. Messel: Ein Pompeji der Paläontologie. Jan Thorbecke, Sigmaringen.
Wang, Y., Cerling, T.E., 1994. A model of fossil tooth and bone diagenesis: implications for paleodiet reconstruction from stable isotopes. Palaeogeogr. Palaeoclimatol. Palaeoecol. 107, 281–289.
Weber, J., 1991. Untersuchungen zur Tonmineralführung der Messel-Formation in der Fundstätte Messel (Mittel-Eozän). Cour. Forschungs-Inst. Senckenberg. 139, 71–81.
Weber, J., Hofmann, U., 1982. Kernbohrungen in der eozänen Fossillagerstätte Grube Messel bei Darmstadt. Geol. Abh. Hessen 83, 58.
Wedmann, S., 2005. Annotated taxon-list of the invertebrate animals from the Eocene fossil site Grube Messel near Darmstadt, Germany. Cour. Forschungs-Inst. Senckenberg. 255, 103–110.
Wetzel, R.G., 1983. Limnology. VII-XII Sauders, Philadelphia, New York, Chicago, pp. 1–767.
Wilde, V., 1989. Untersuchungen zur Systematik der Blattreste aus dem Mitteleozän der Grube Messel bei Darmstadt (Hessen, Bundesrepublik Deutschland). Cour. Forschungs-Inst. Senckenberg. 115, 1–212.
Wilde, V., 2004. Aktuelle Übersicht zur Flora aus dem mitteleozänen "Ölschiefer" der Grube Messel bei Darmstadt (Hessen, Deutschland). Cour. Forschungs-Inst. Senckenberg. 252, 109–114.
Wilde, V., Hellmund, M., 2010. First record of gut contents from a middle Eocene equid form the Geiseltal near Halle (Saale), Sachsen-Anhalt, Central Germany. Palaeobiodivers. Palaeoenviron. 90, 153–162.
Wuttke, M., 1983. "Weichteil-Erhaltung" durch lithifizierte Mikroorganismen bei mitteleozänen Vertebraten aus den Ölschiefern der "Grube Messel" bei Darmstadt. Senckenb. Lethaea 64, 509–527.
Wuttke, M., 1992. Conservation–dissolution–transformation. On the behaviour of biogenic materials during fossilization. In: Schaal, S., Ziegler, W. (Eds.), Messel—An Insight Into the History of Life and of the Earth. Clarendon, Oxford, pp. 263–275.
Yakir, D., 1997. Oxygen-18 of leaf water: a crossroad for plant associated isotopic signals. In: Griffiths, H. (Ed.), Stable Isotopes: Integration of Biological, Ecological and Geochemical Processes. BIOS, Oxford, pp. 147–168.
Zazzo, A., Lécuyer, C., Mariotti, A., 2004. Experimentally-controlled carbon and oxygen isotope exchange between bioapatites and water under inorganic and microbially-mediated conditions. Geochim. Cosmochim. Acta 68, 1–12.